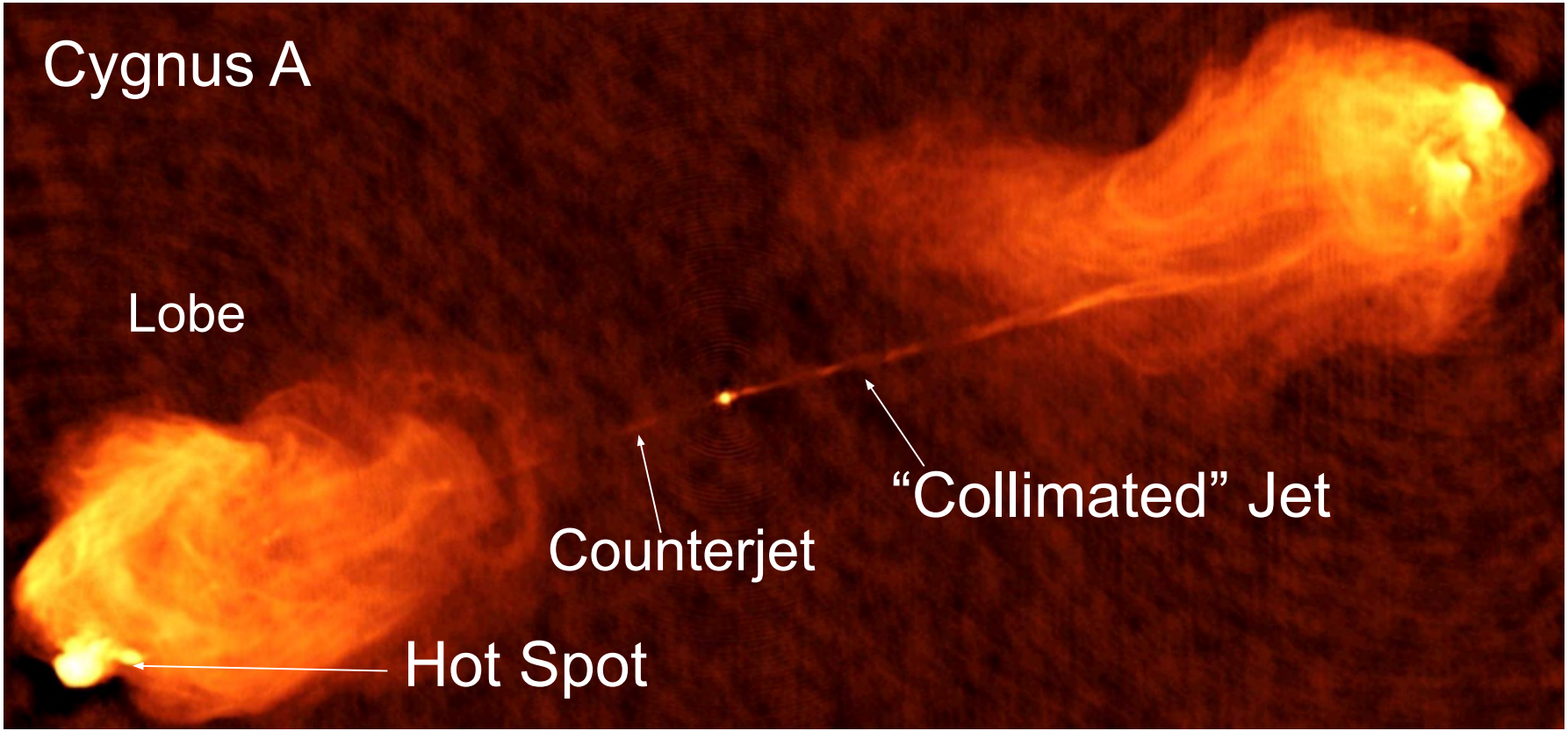
# A Magnetic Helix at the Heart of M87: New Polarization Insights Challenging Jet Formation Theory

December 12, 2025

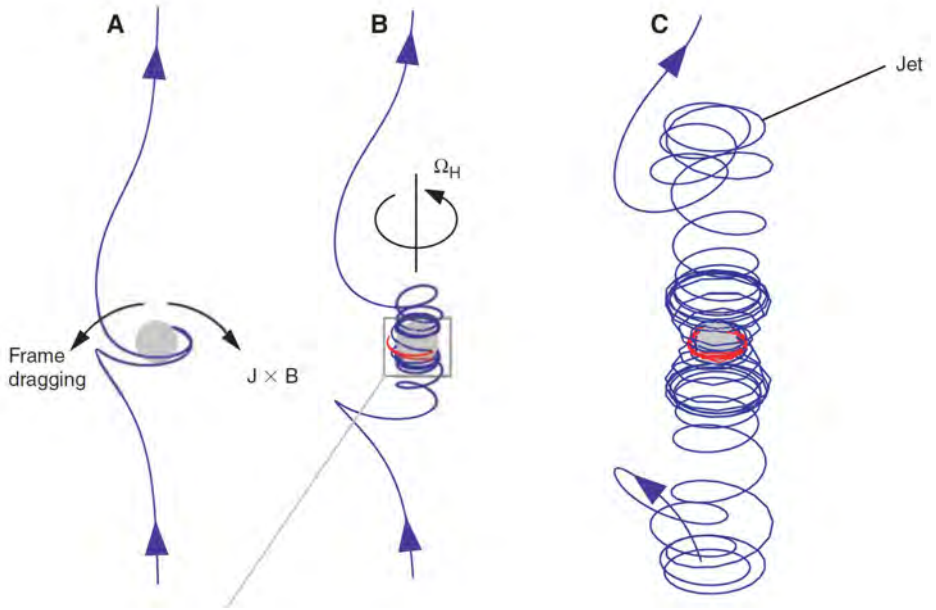
Presenter: Jongho Park (Kyung Hee University)
on behalf of the project team

# Relativistic Jets in Active Galactic Nuclei



# Jet Launching

**The Blandford-Znajek Mechanism**



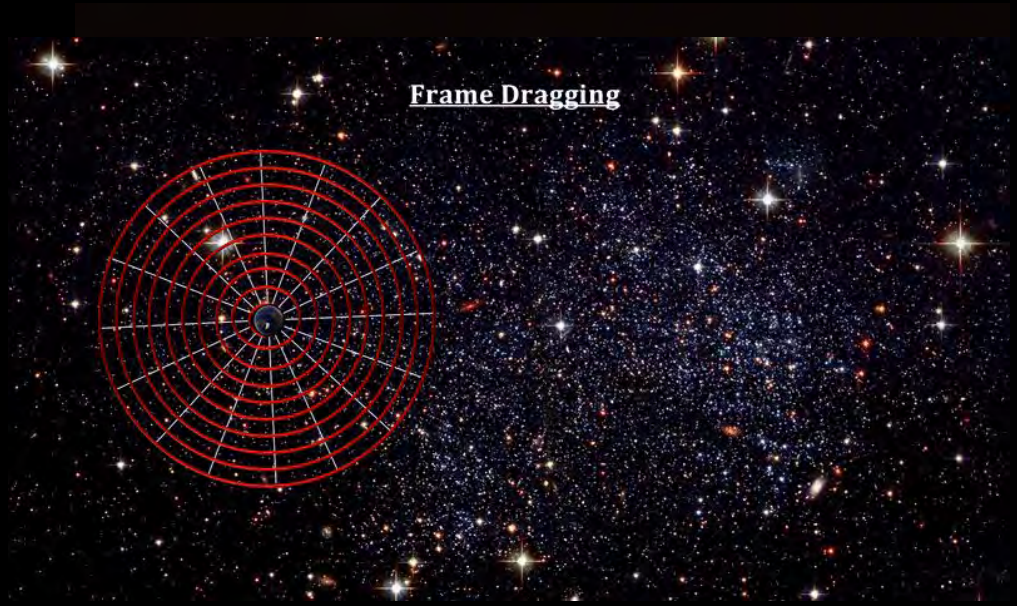

Narayan & Quataert (2005)

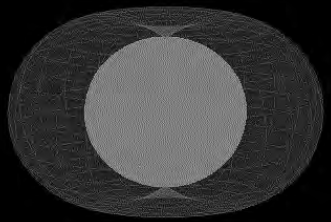
- Relativistic AGN jets are believed to be launched by the magnetic field twisted by the frame-dragging effect of the spinning black hole.

- During this process, the rotational energy of the black hole can be extracted and used to power the jet (the **Blandford-Znajek** process).

# Doppler Boosting and Brightness Asymmetry

Semenov (2005)

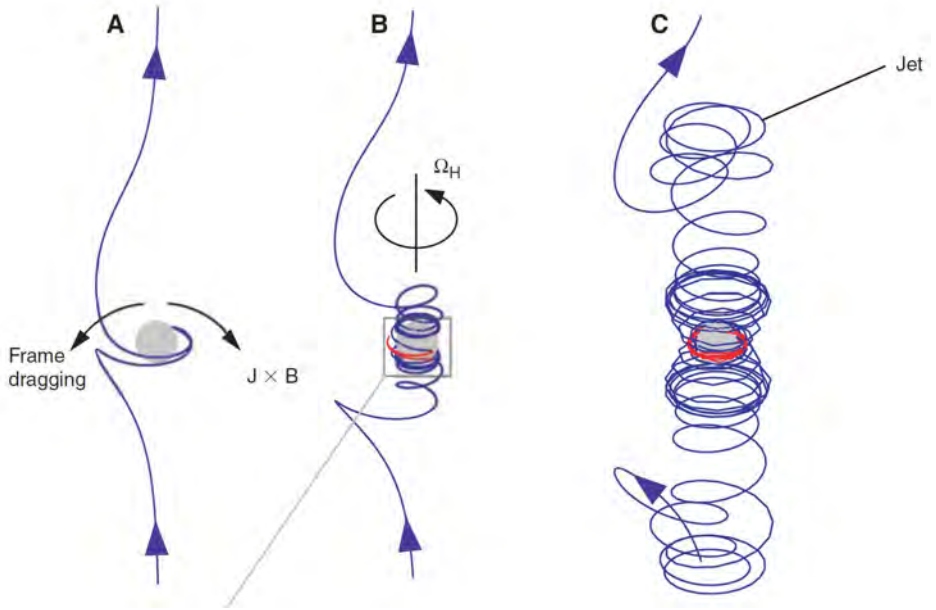


The frame-dragging and Doppler boosting effects.

# Jet Launching

**The Blandford-Znajek Mechanism**



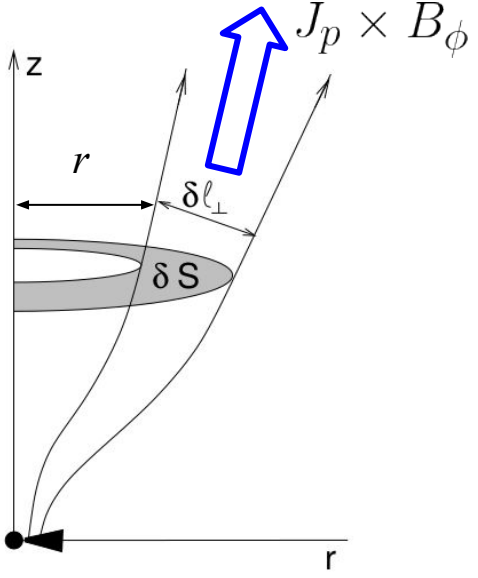

Narayan & Quataert (2005)

- Relativistic AGN jets are believed to be launched by the magnetic field twisted by the frame-dragging effect of the spinning black hole.

- During this process, the rotational energy of the black hole can be extracted and used to power the jet (the **Blandford-Znajek** process).

# Jet Collimation & Acceleration

## Magnetic (or MHD) Jet Acceleration Model




Vlahakis (2015)

$$\text{Total Energy Flux} \approx \text{Poynting Flux} + \text{Kinetic Energy Flux}$$

$$\frac{\text{Poynting flux}}{\text{Total energy flux}} \propto r^2 B_p$$

$$B_p \delta S = \text{const} \qquad \delta S = r \delta l_\perp$$

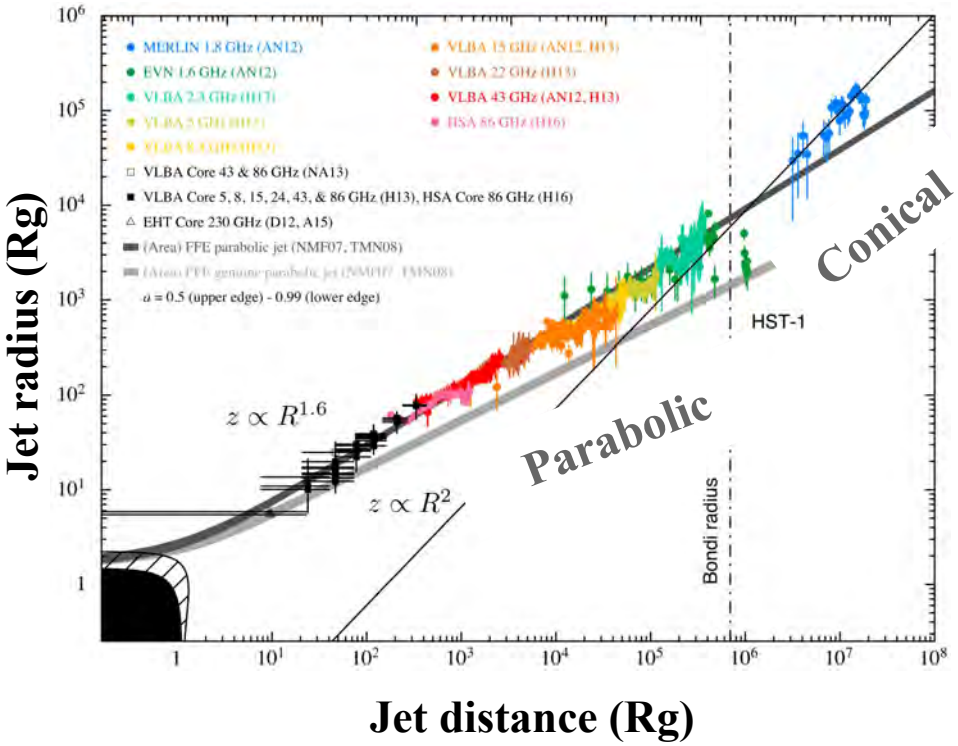
$$\frac{\text{Poynting flux}}{\text{Total energy flux}} \propto \frac{r}{\delta l_\perp}$$

**Differential Collimation** of Poloidal Field Lines
: Inner field lines are more collimated than outer field lines

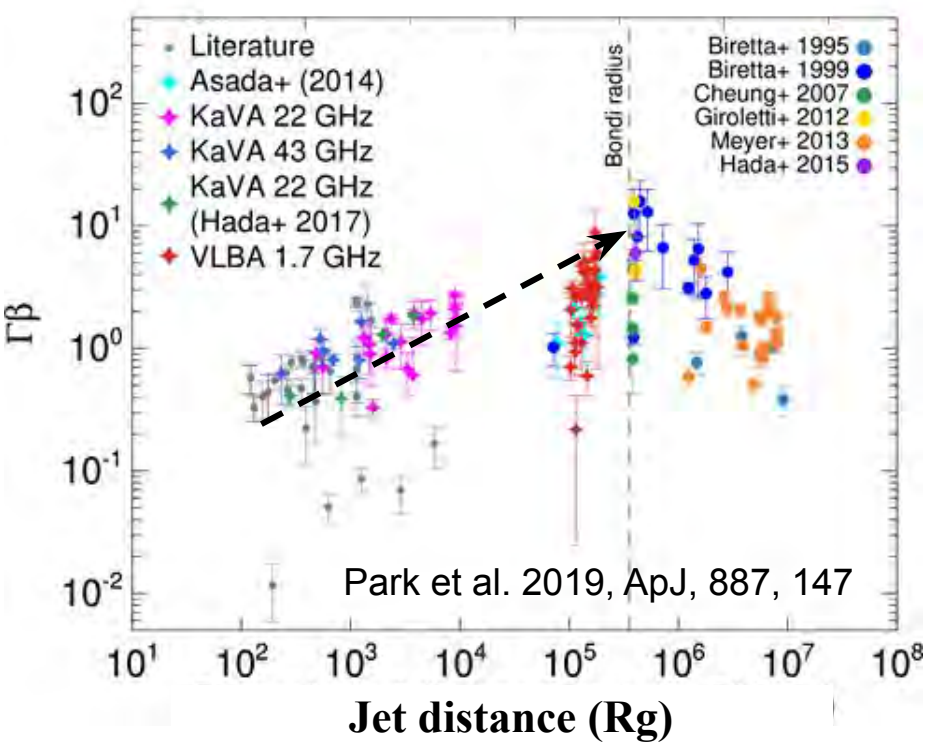
→ The jet acceleration is expected to be efficient when the jet is systematically collimated!

# Jet Collimation & Acceleration - M87 (FR I)

## Jet Collimation

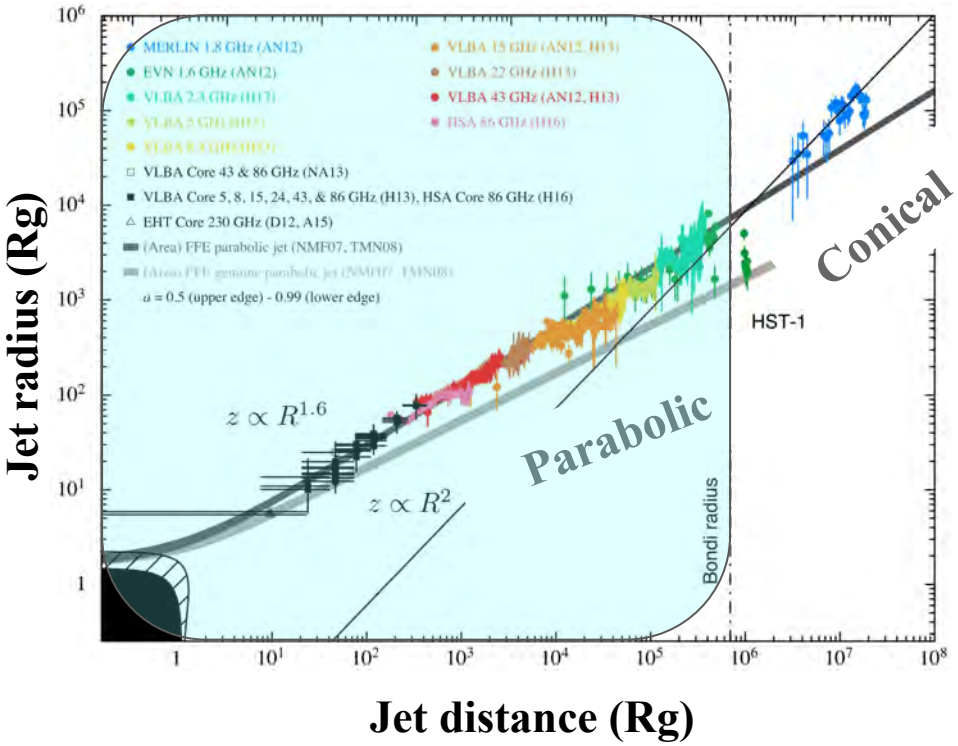



## Jet Acceleration

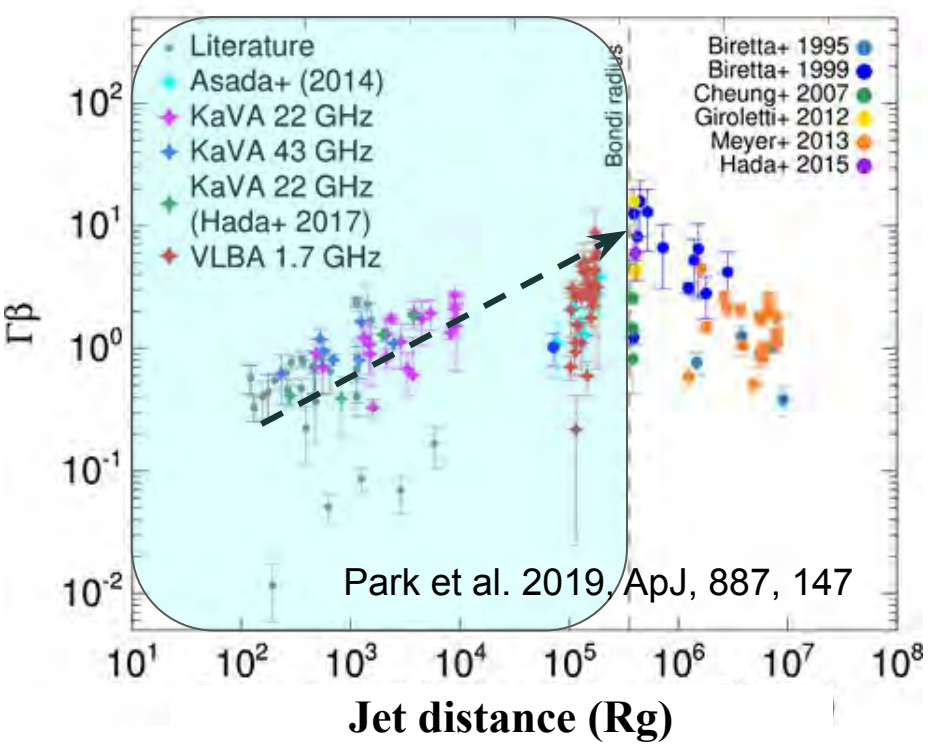


# Jet Collimation & Acceleration - M87 (FR I)

## Jet Collimation

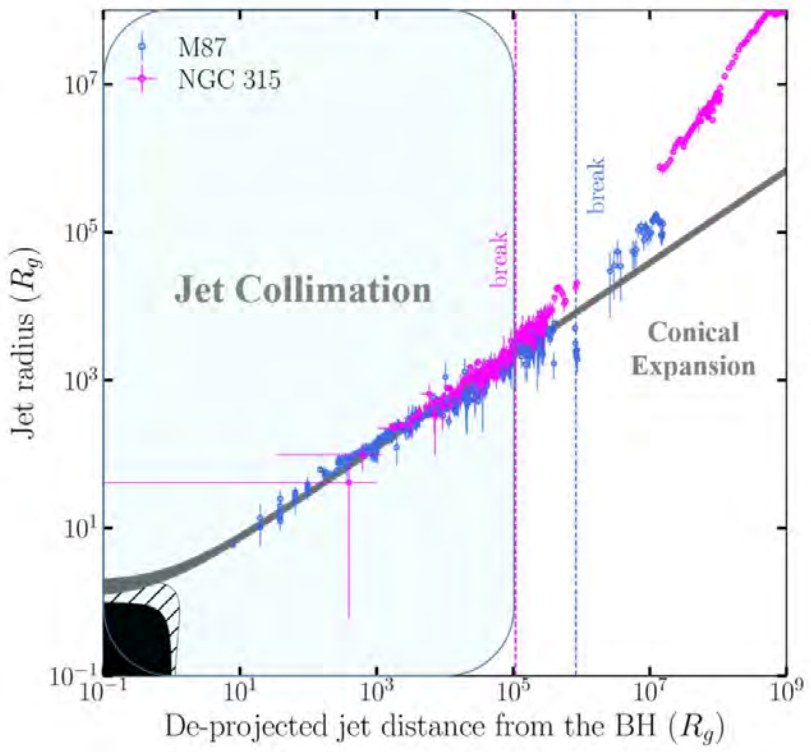


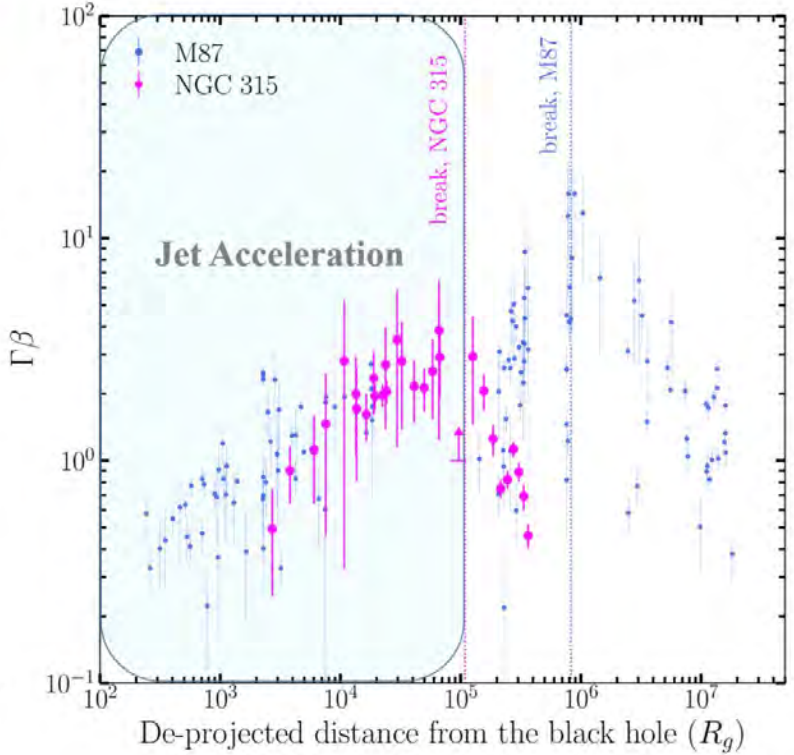

## Jet Acceleration



# Jet Collimation & Acceleration - NGC 315 (FR I)

Park et al. 2021, ApJ, 909, 76



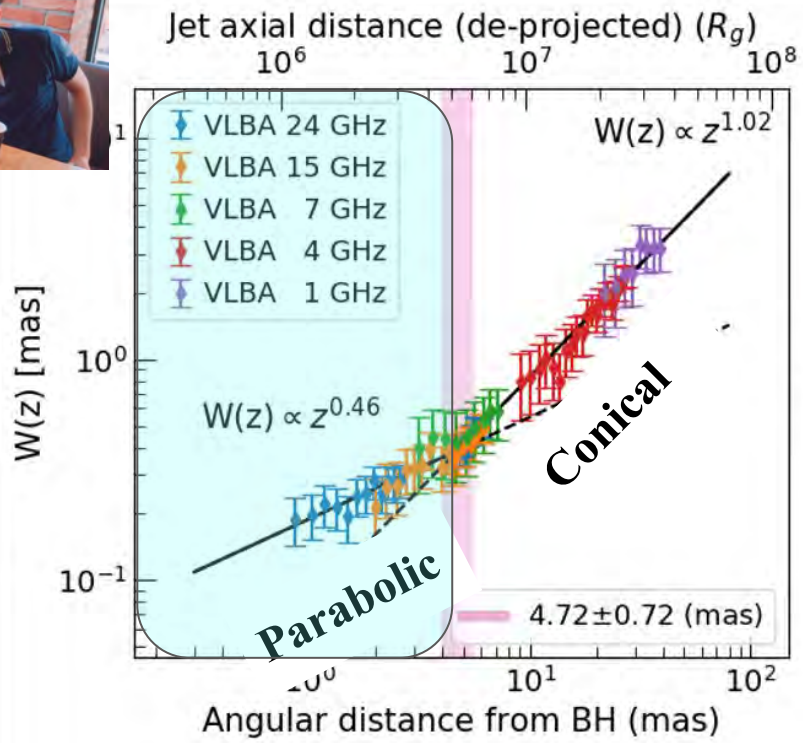



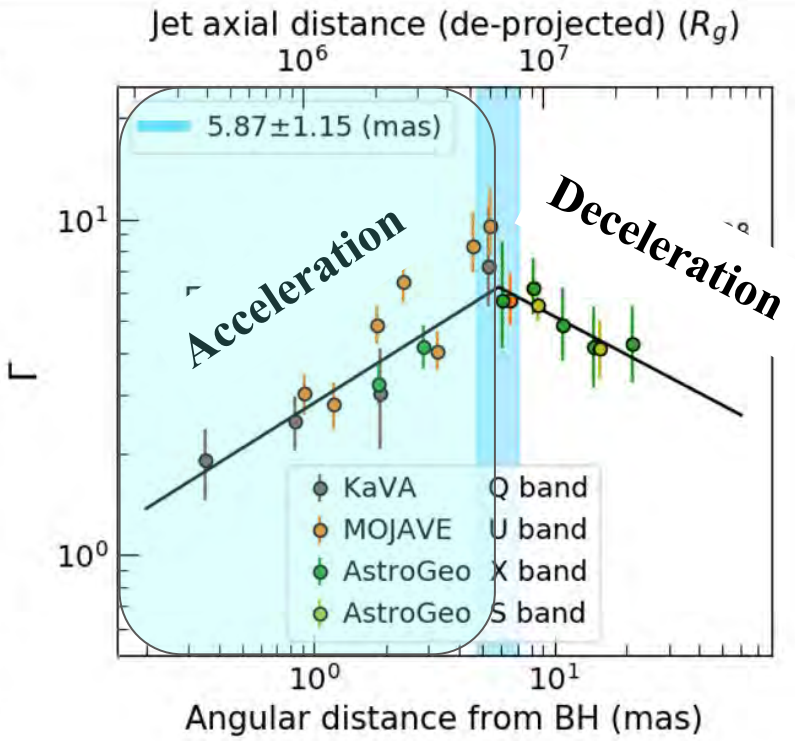
# Jet Collimation & Acceleration - 1928+738 (Quasar)



Kunwoo Yi at Kyung Hee University

Yi, Park, et al. 2024, A&A, 688, 94



# Jet Collimation & Acceleration - 1928+738 (Quasar)



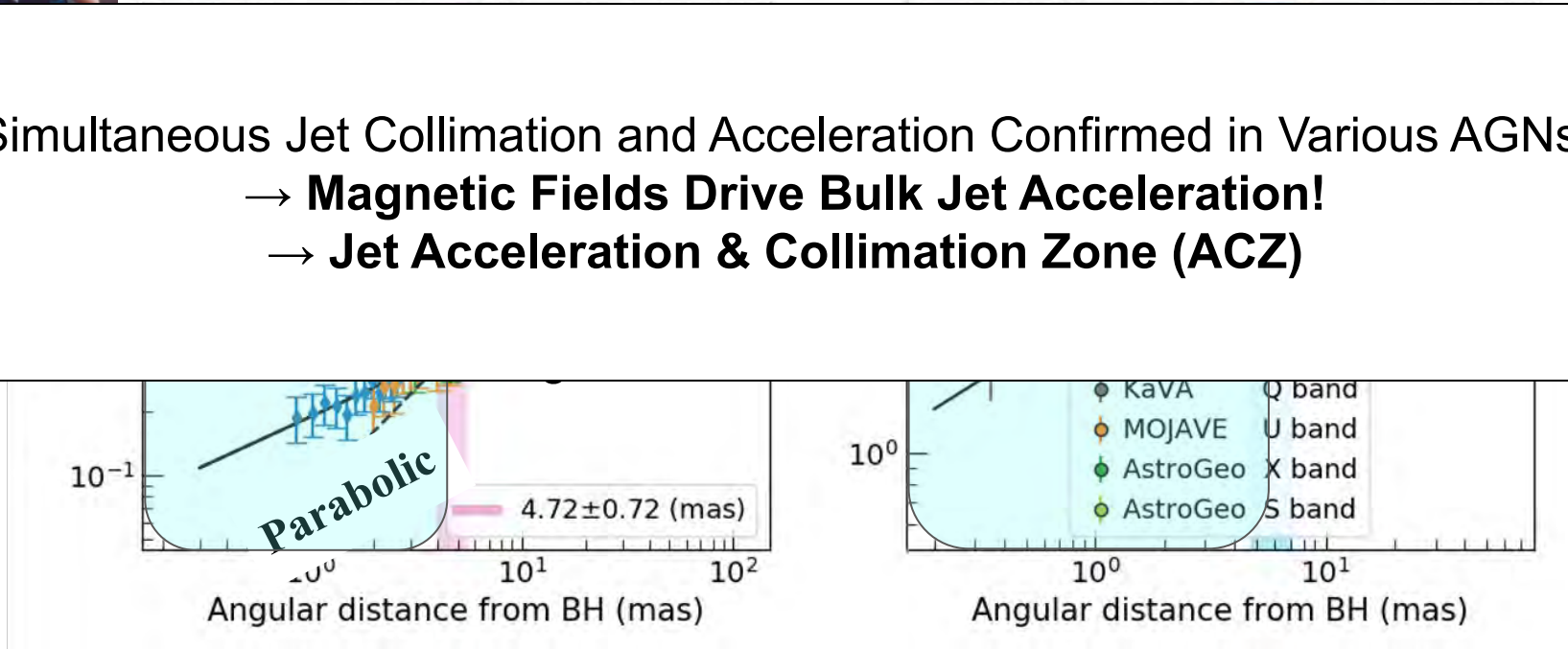
Kunwoo Yi at Kyung Hee University

Yi, Park, et al. 2024, A&A, 688, 94

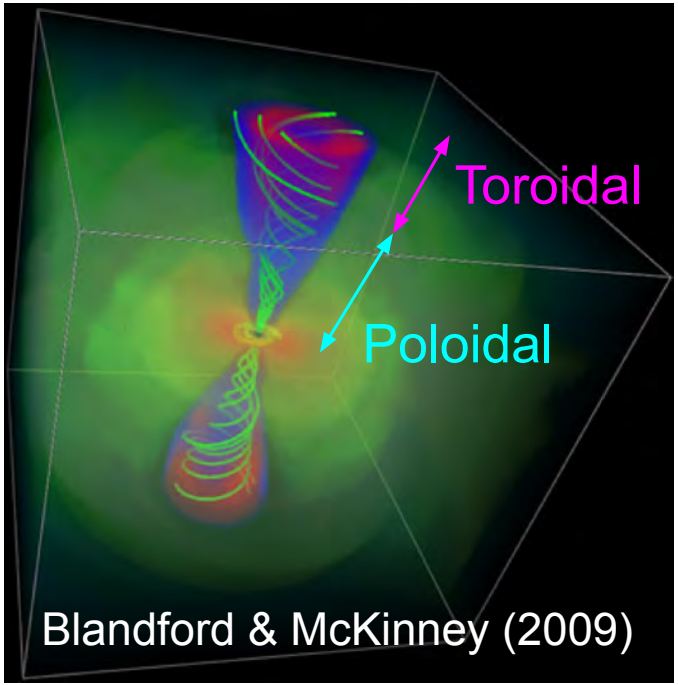
Simultaneous Jet Collimation and Acceleration Confirmed in Various AGNs.

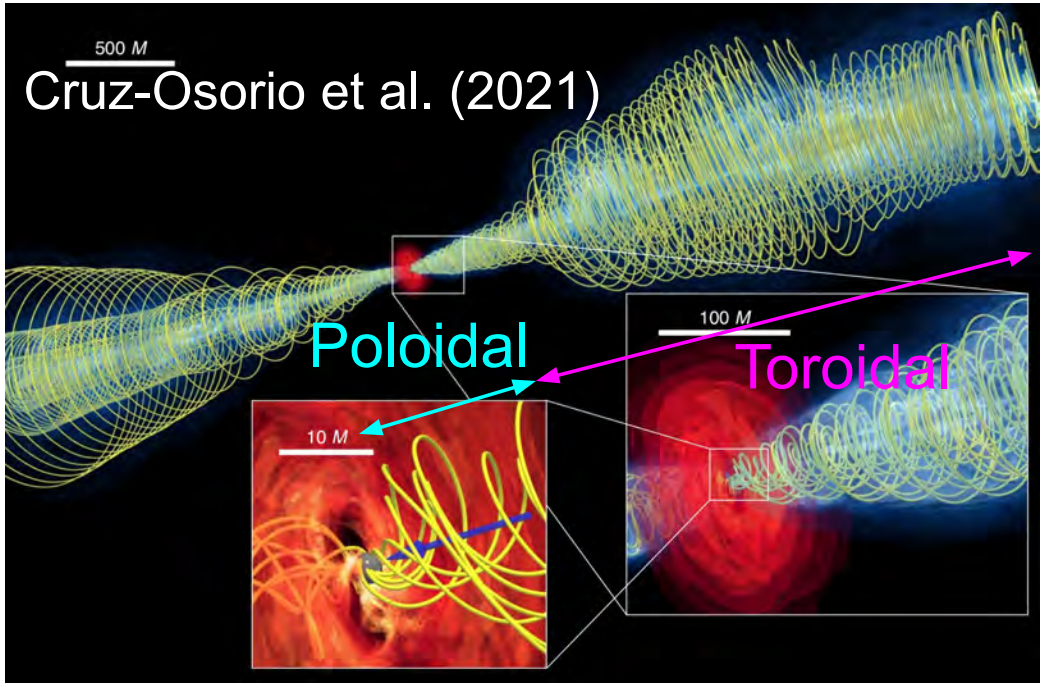
→ **Magnetic Fields Drive Bulk Jet Acceleration!**

→ **Jet Acceleration & Collimation Zone (ACZ)**



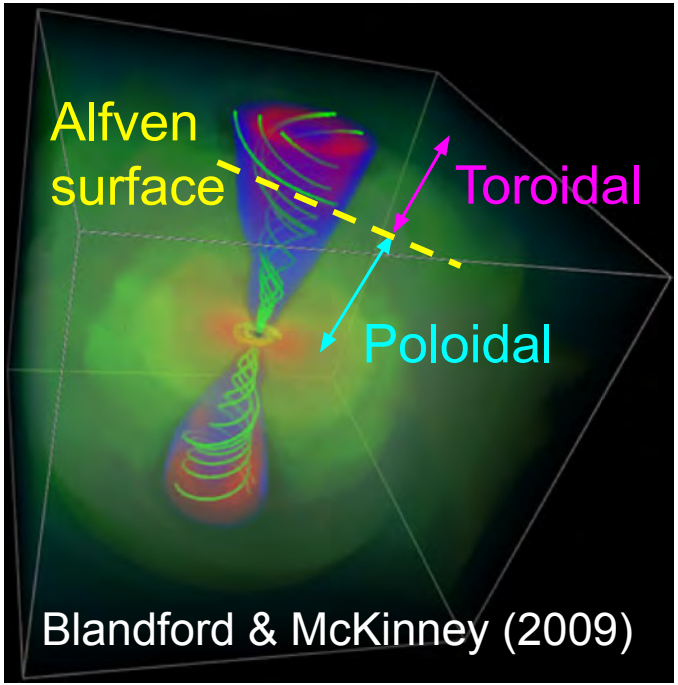
# Theory Prediction: Poloidal to Toroidal B-Field Transition

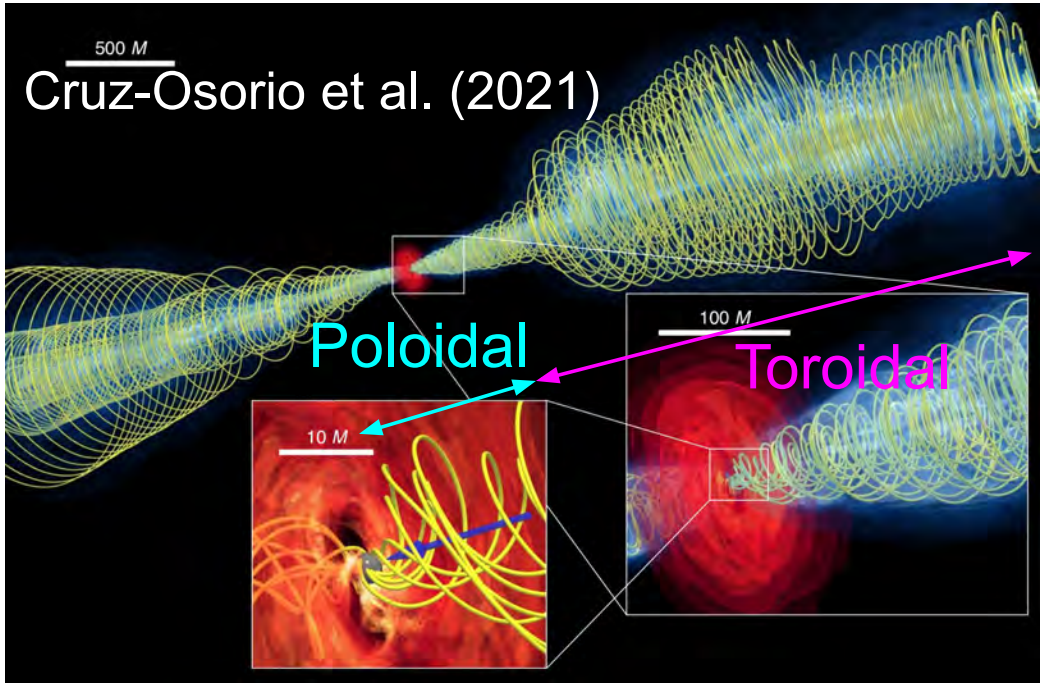



Current MHD theory predicts a **toroidal-dominated B-field** structure in most of the ACZ regions of AGNs.

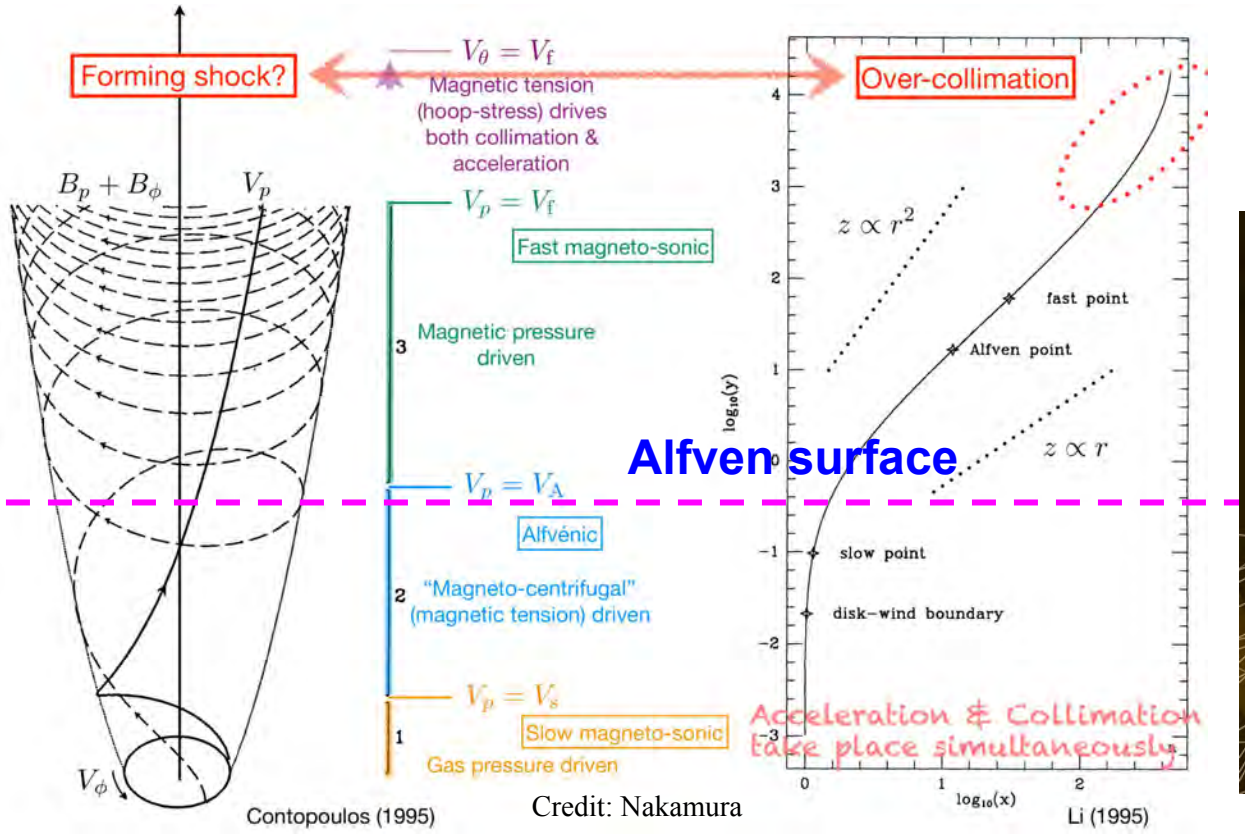
# Theory Prediction: Poloidal to Toroidal B-Field Transition



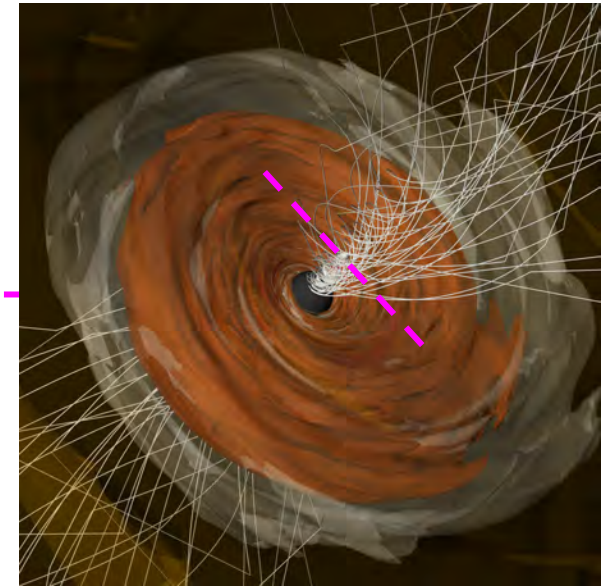

Current MHD theory predicts a **toroidal-dominated B-field** structure in most of the ACZ regions of AGNs.

# Theory Prediction: Poloidal to Toroidal B-Field Transition

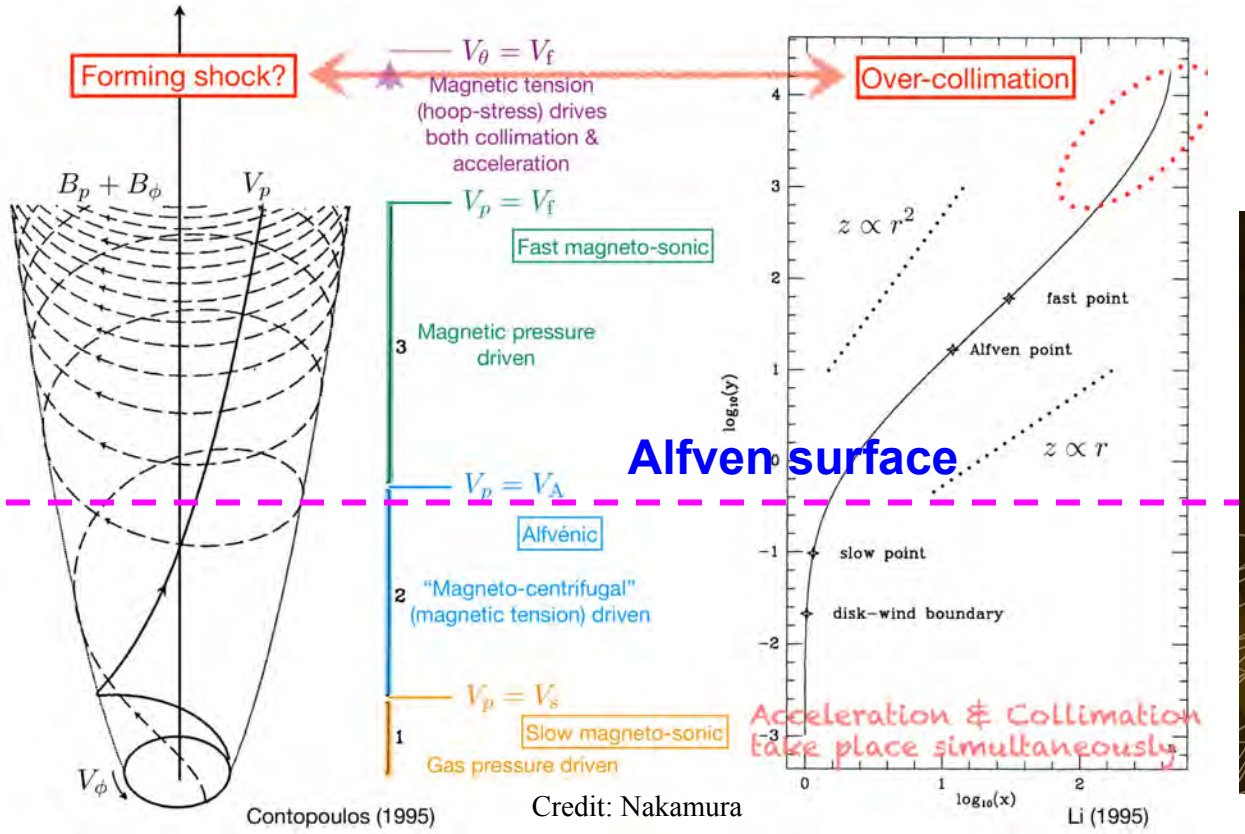



Credit: Nakamura

$$\frac{B_\phi}{B_p} \simeq -\frac{\Omega_F R - v_\phi}{v_p} \approx -\frac{\Omega_F R}{v_p}$$

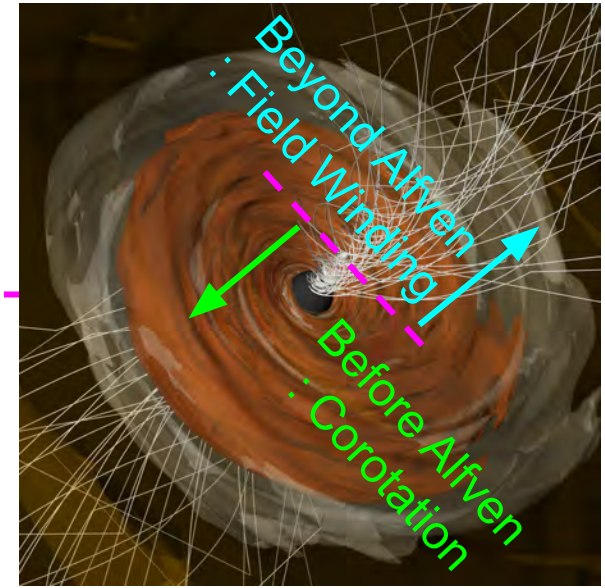


# Theory Prediction: Poloidal to Toroidal B-Field Transition

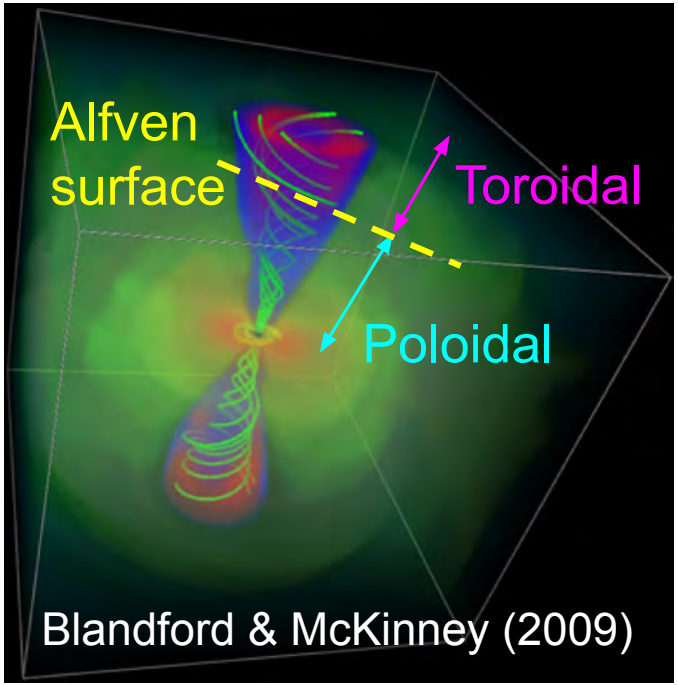


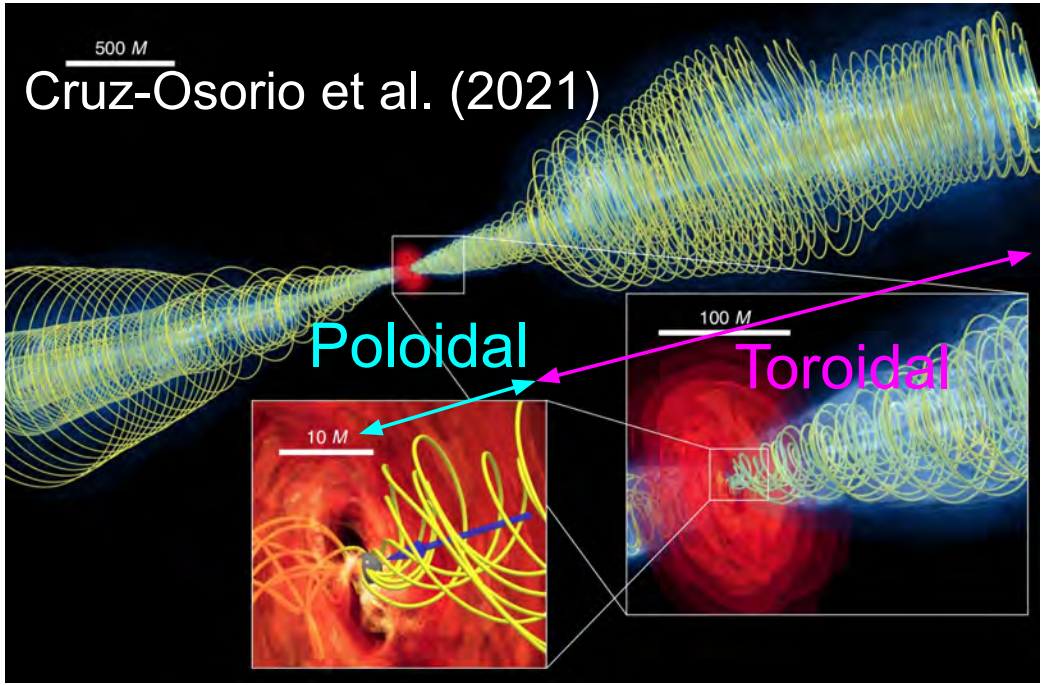

Credit: Nakamura

$$\frac{B_\phi}{B_p} \simeq -\frac{\Omega_F R - v_\phi}{v_p} \approx -\frac{\Omega_F R}{v_p}$$



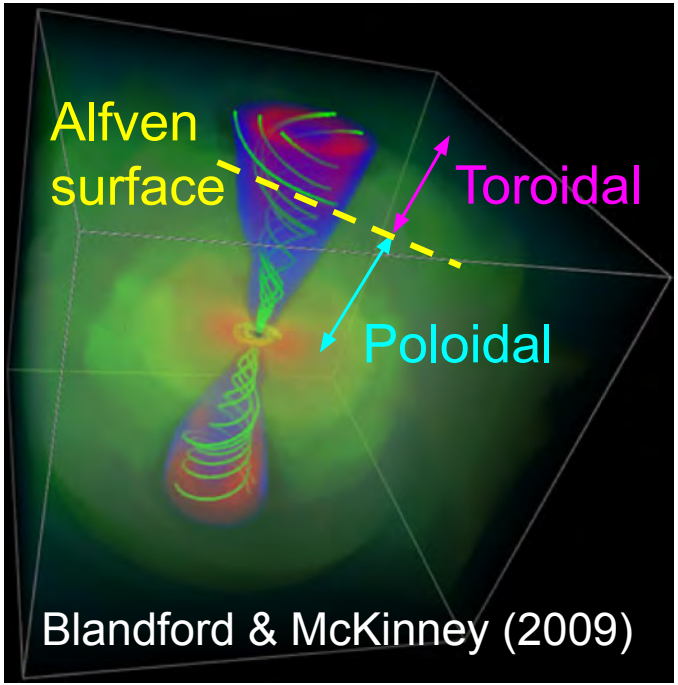
# Theory Prediction: Poloidal to Toroidal B-Field Transition

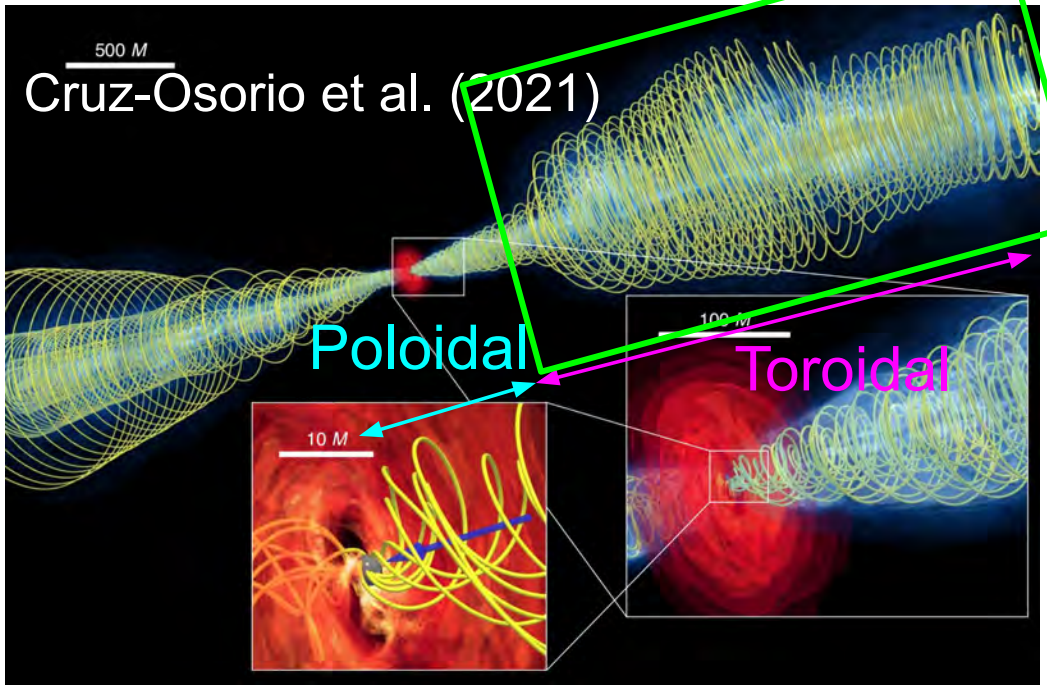



Current MHD theory predicts a **toroidal-dominated B-field** structure in most of the ACZ regions of AGNs.

# Theory Prediction: Poloidal to Toroidal B-Field Transition




Current MHD theory predicts a **toroidal-dominated B-field** structure in most of the ACZ regions of AGNs.

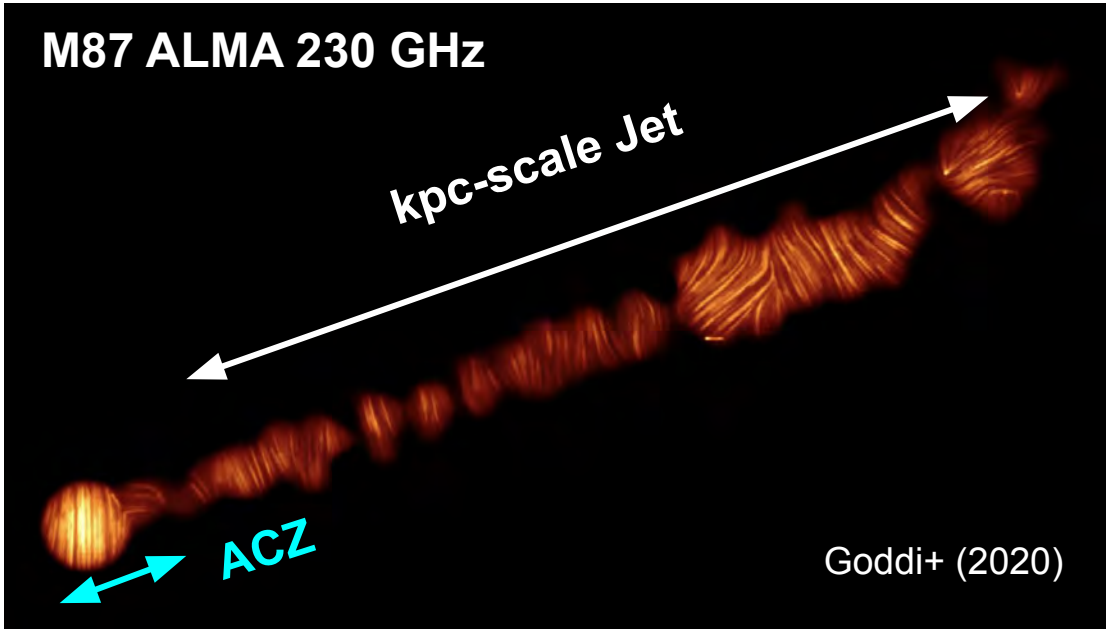
**Magnetic fields drive the launching, collimation, and acceleration of AGN jets.**

**Why is the B-field structure so hard to constrain observationally?**

# Magnetic Field in the Jet Acceleration & Collimation Zone (ACZ)

Several **Challenges** in Constraining the Magnetic Field Structure in the ACZs.

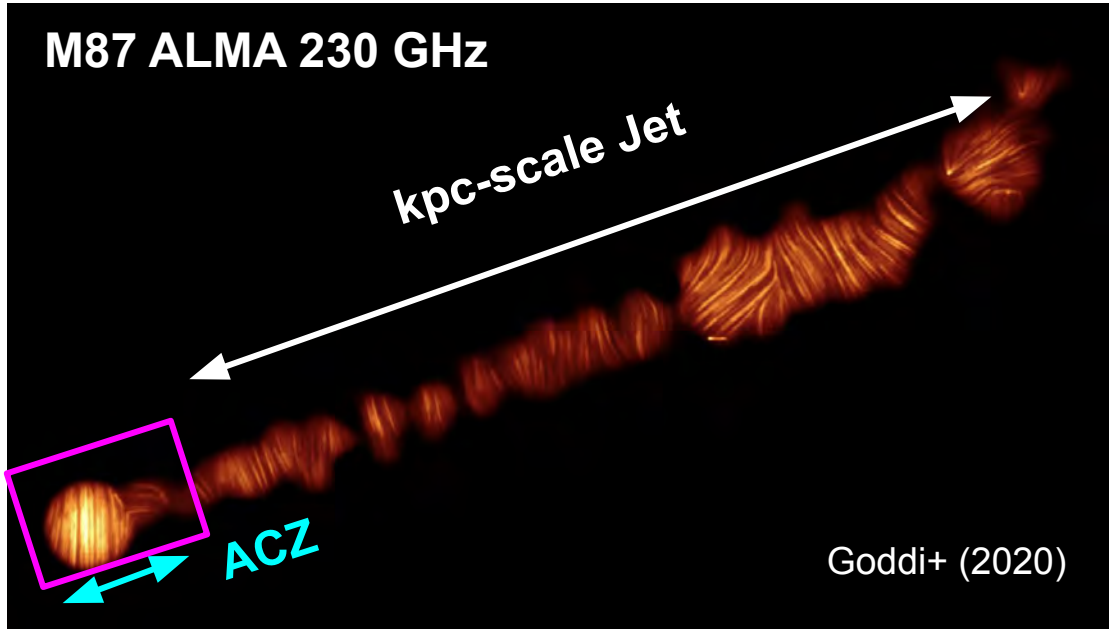
1. The jet is very weakly polarized or unpolarized in the ACZs.



# Magnetic Field in the Jet Acceleration & Collimation Zone (ACZ)

Several **Challenges** in Constraining the Magnetic Field Structure in the ACZs.

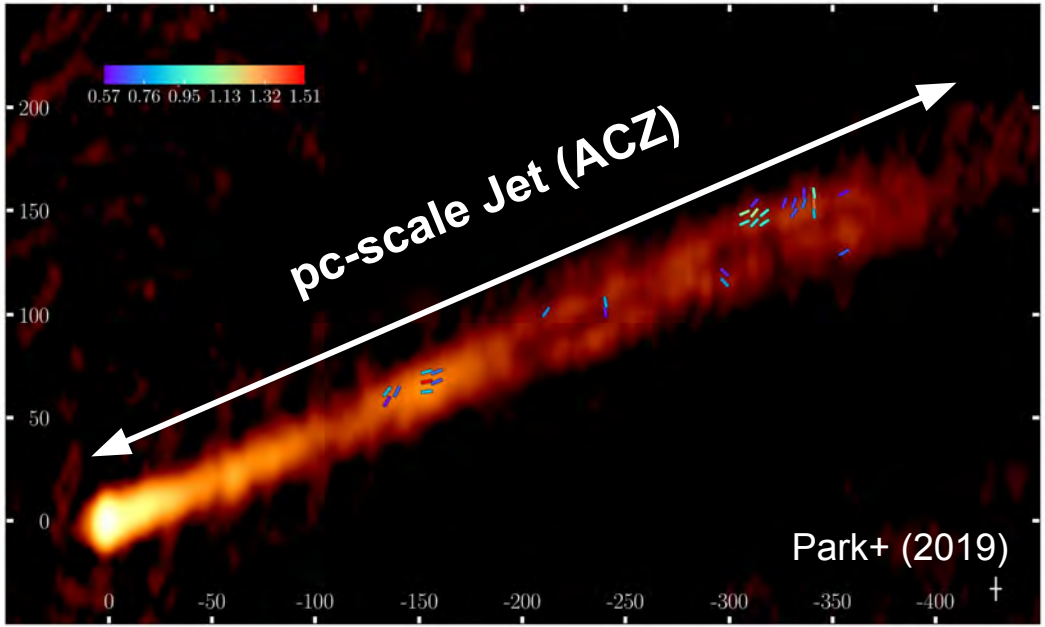
1. The jet is very weakly polarized or unpolarized in the ACZs.



# Magnetic Field in the Jet Acceleration & Collimation Zone (ACZ)

Several **Challenges** in Constraining the Magnetic Field Structure in the ACZs.

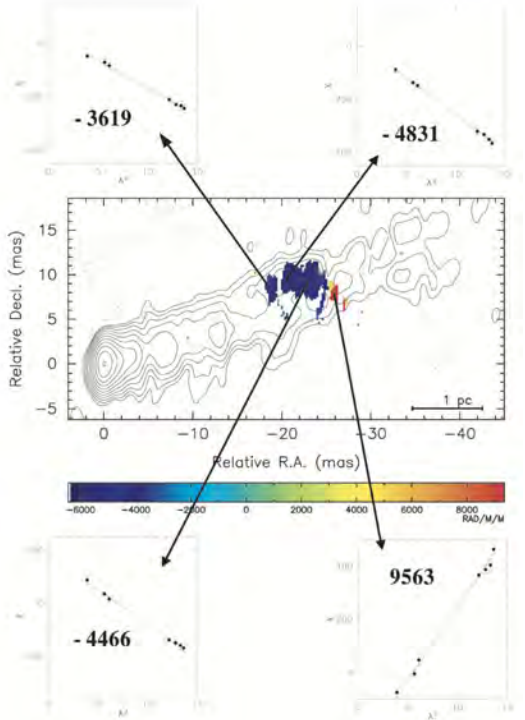
1. The jet is very weakly polarized or unpolarized in the ACZs.



# Magnetic Field in the Jet Acceleration & Collimation Zone (ACZ)

Several **Challenges** in Constraining the Magnetic Field Structure in the ACZs.

2. Even when linearly polarized emission is detected, significant external Faraday rotation is common.
   → Thus, the intrinsic EVPA—and hence the magnetic-field geometry—can only be obtained after RM correction.

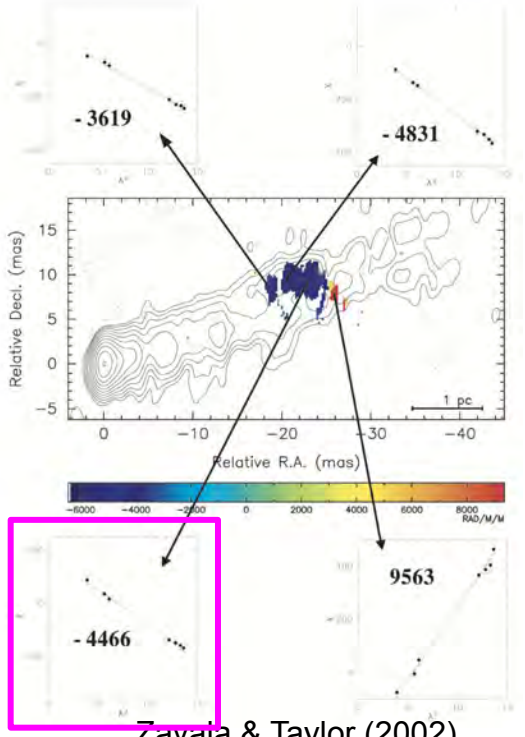



Zavala & Taylor (2002)

# Magnetic Field in the Jet Acceleration & Collimation Zone (ACZ)

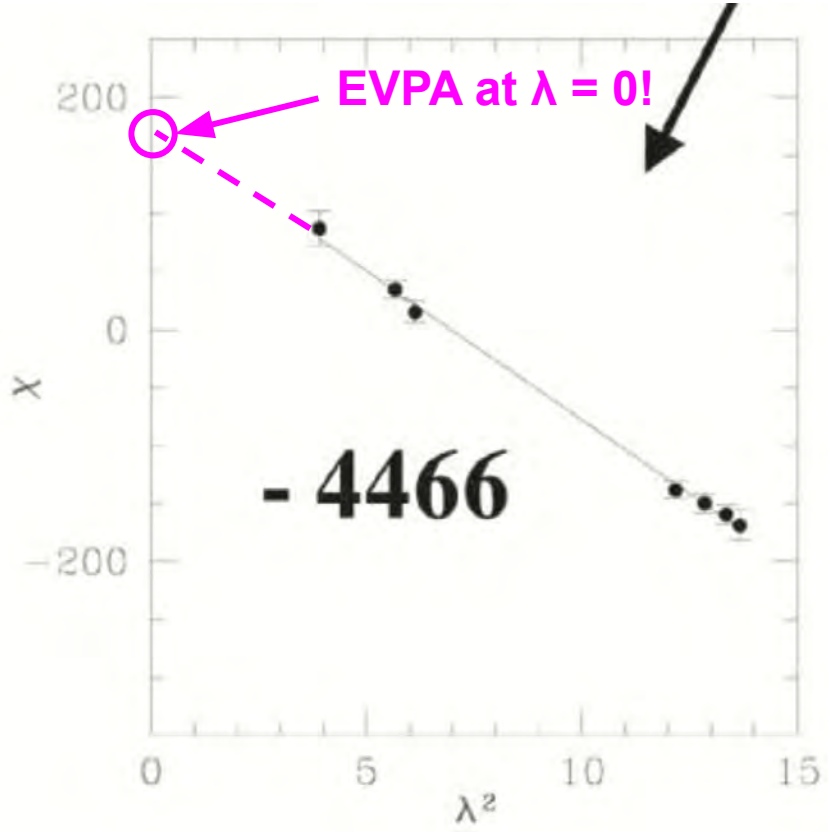
Several **Challenges** in Constraining the Magnetic Field Structure in the ACZs.

2. Even when linearly polarized emission is detected, significant external Faraday rotation is common.
   → Thus, the intrinsic EVPA—and hence the magnetic-field geometry—can only be obtained after RM correction.

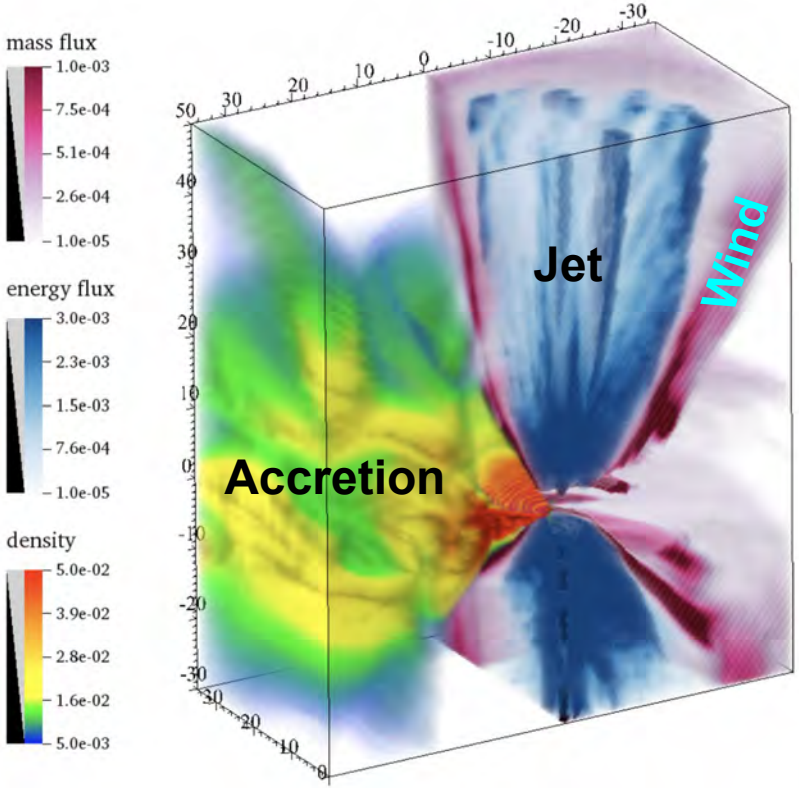


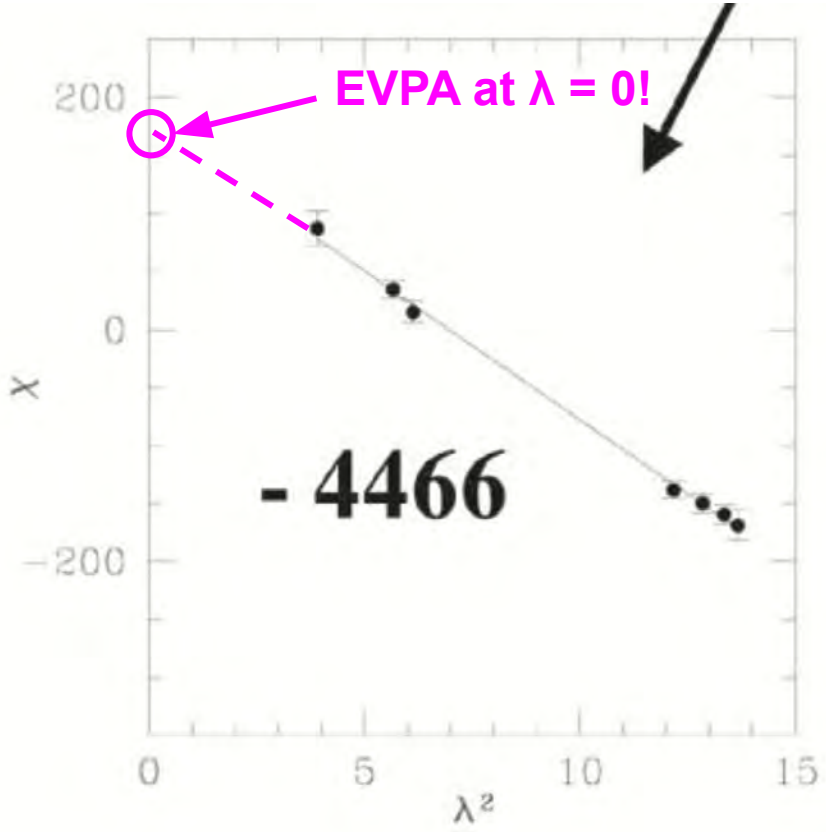

Zavala & Taylor (2002)

# Magnetic Field in the Jet Acceleration & Collimation Zone (ACZ)



# Magnetic Field in the Jet Acceleration & Collimation Zone (ACZ)

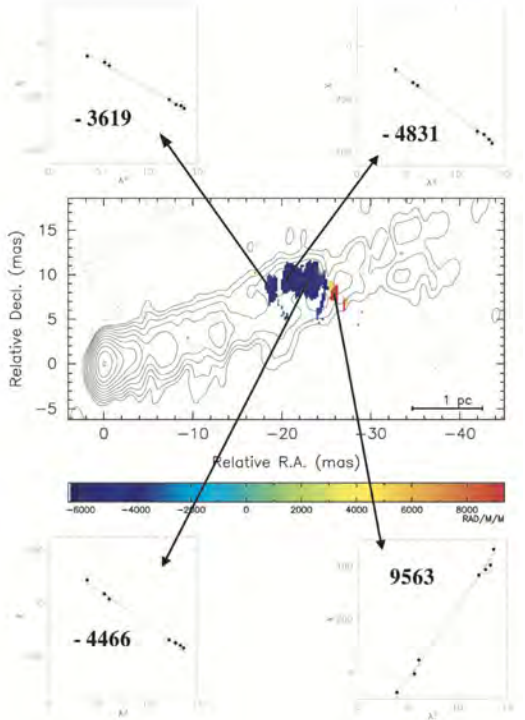


# Magnetic Field in the Jet Acceleration & Collimation Zone (ACZ)

Several **Challenges** in Constraining the Magnetic Field Structure in the ACZs.

2. Even when linearly polarized emission is detected, significant external Faraday rotation is common.
   → Thus, the intrinsic EVPA—and hence the magnetic-field geometry—can only be obtained after RM correction.




Zavala & Taylor (2002)

# Magnetic Field in the Jet Acceleration & Collimation Zone (ACZ)

Several **Challenges** in Constraining the Magnetic Field Structure in the ACZs.

3. Because of relativistic aberration and projection, the jet's observed linear-polarization pattern is not a simple 90 degrees tracer of the intrinsic magnetic-field geometry.
   → We need a forward-modeling approach to infer the jet's magnetic-field structure.

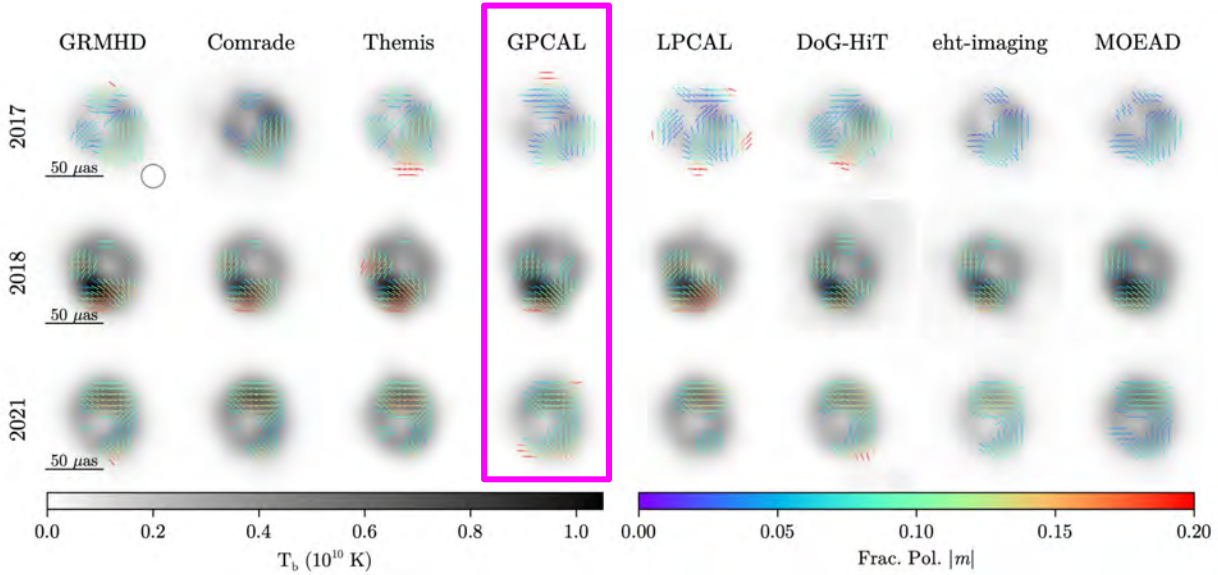
# Magnetic Field in the Jet Acceleration & Collimation Zone (ACZ)

How did we overcome the **Challenges**?

1. Weak Jet Polarization in the ACZs.
   → High Sensitivity Array (HSA; VLBA + phased VLA + Effelsberg 100m).
   → Development of a Dedicated Calibration Pipeline **'GPCAL'**.
2. Large External Faraday Rotation in the ACZs.
   → Multifrequency (**22 Bands**,1.4 - 24.4 GHz) Observations for RM correction.
3. Relativistic Aberration & Projection Effects.
   → **Forward modeling** with relativistic MHD and polarized radiative transfer.

The Event Horizon Telescope Collaboration et al. (2025)



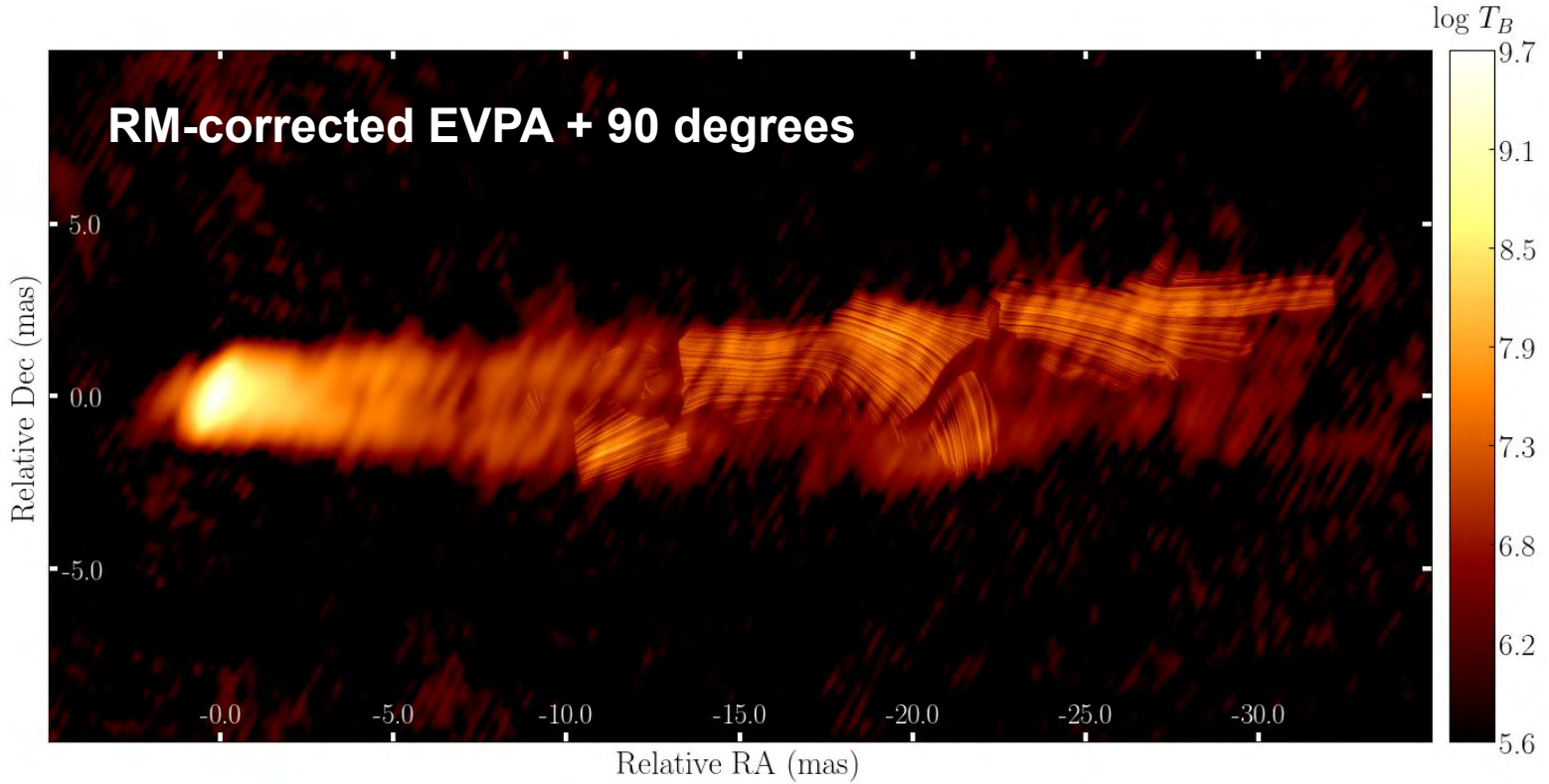



# Magnetic Field in the Jet Acceleration & Collimation Zone (ACZ)

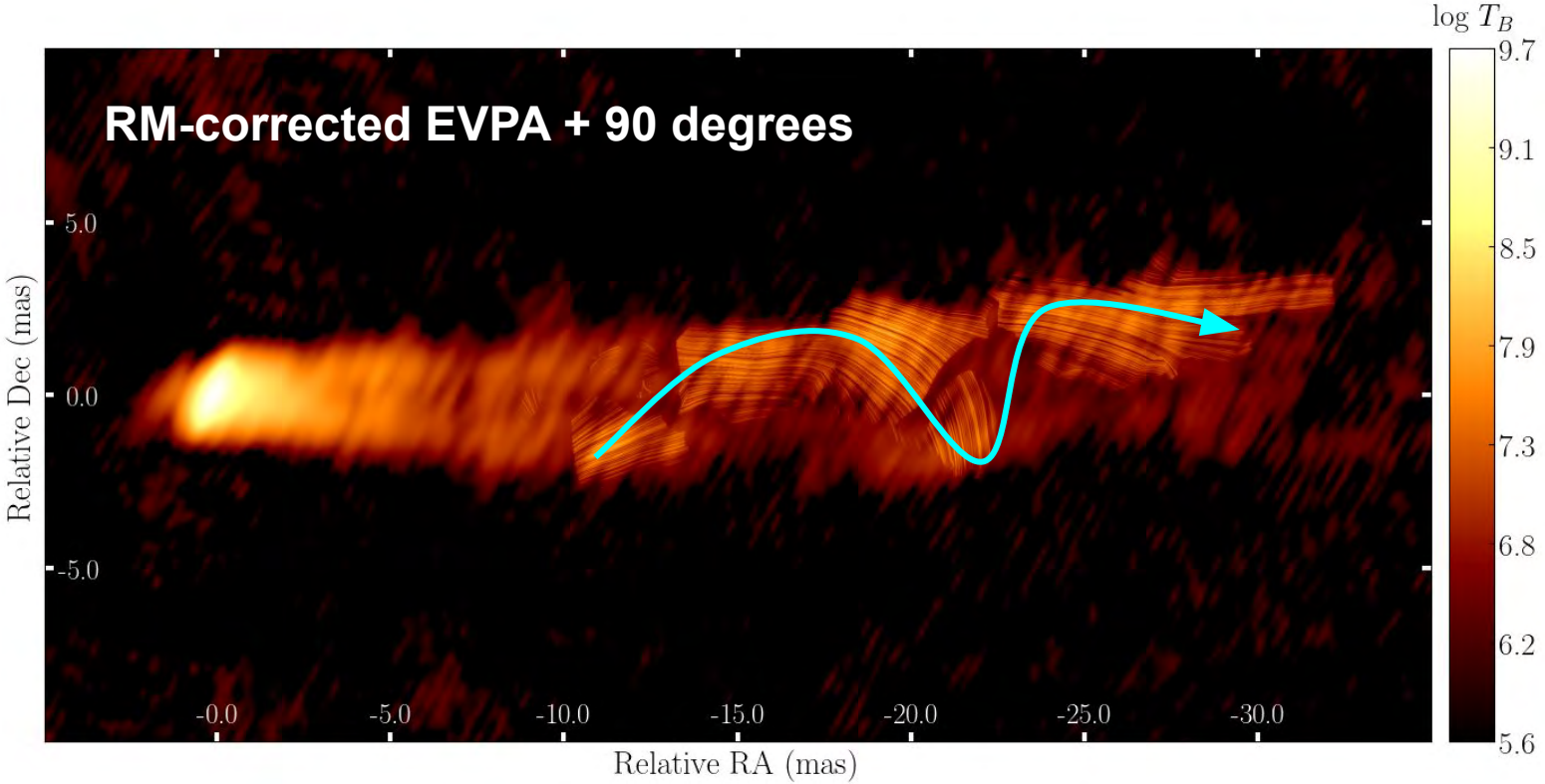
How did we overcome the **Challenges**?

1. Weak Jet Polarization in the ACZs.
   → High Sensitivity Array (HSA; VLBA + phased VLA + Effelsberg 100m).
   → Development of a Dedicated Calibration Pipeline **'GPCAL'**.
2. Large External Faraday Rotation in the ACZs.
   → Multifrequency (**22 Bands**,1.4 - 24.4 GHz) Observations for RM correction.
3. Relativistic Aberration & Projection Effects.
   → **Forward modeling** with relativistic MHD and polarized radiative transfer.

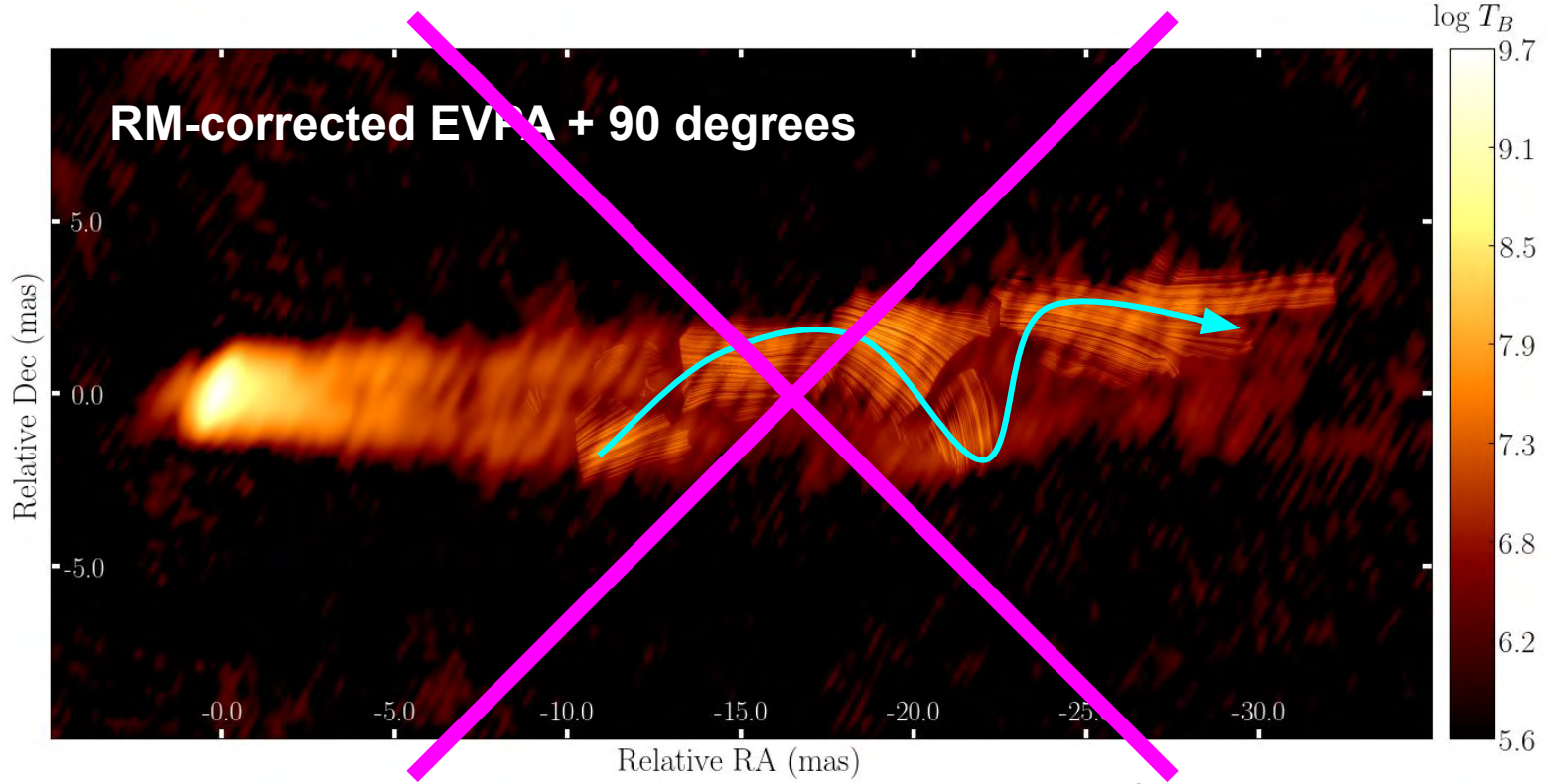
# Results


RM-corrected EVPA + 90 degrees
log $T_B$
9.7
9.1
8.5
7.9
7.3
6.8
6.2
5.6
5.0
0.0
-5.0
Relative Dec (mas)
-0.0
-5.0
-10.0
-15.0
-20.0
-25.0
-30.0
Relative RA (mas)

# Results

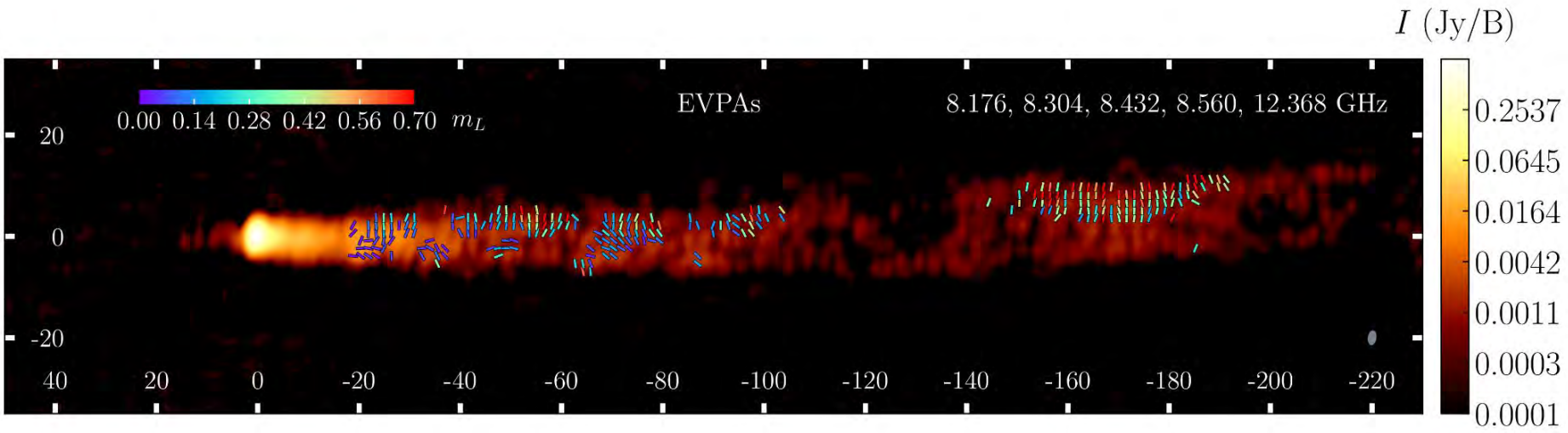

RM-corrected EVPA + 90 degrees
log $T_B$
9.7
9.1
8.5
7.9
7.3
6.8
6.2
5.6
5.0
0.0
-5.0
Relative Dec (mas)
-0.0
-5.0
-10.0
-15.0
-20.0
-25.0
-30.0
Relative RA (mas)

# Results




**The observed E-vectors are already Lorentz-Transformed!**

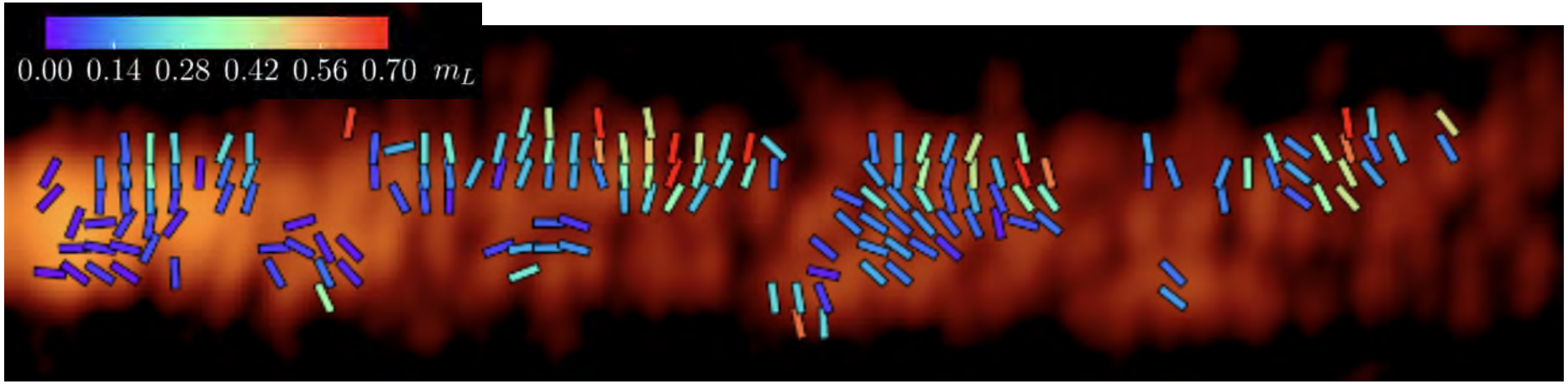
# Results




In the Far Zone (between ≈ 2e4 and ≈ 2e5 Rg)

- North : EVPAs Perpendicular to the Jet Axis.
- South : EVPAs Either Parallel or Perpendicular to the Jet Axis.
- Higher Fractional Linear Polarization in the North Limb than the South Limb.

# Results



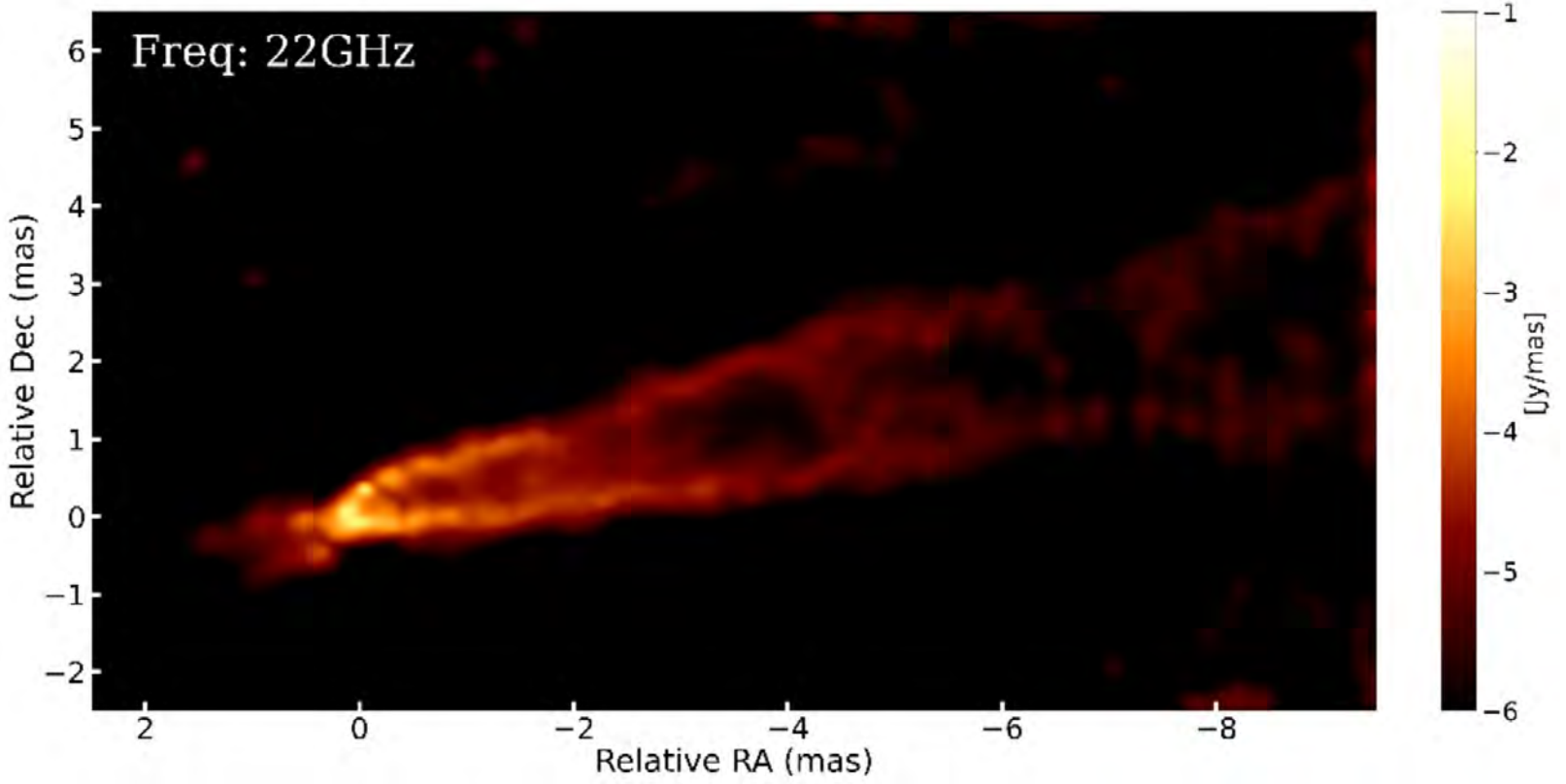

-20 mas -100 mas

In the Far Zone (between ≈ 2e4 and ≈ 2e5 Rg)

- North : EVPAs Perpendicular to the Jet Axis.
- South : EVPAs Either Parallel or Perpendicular to the Jet Axis.
- Higher Fractional Linear Polarization in the North Limb than the South Limb.

# Edge-Brightened Jet in M87

Poster  Imkwang Kang

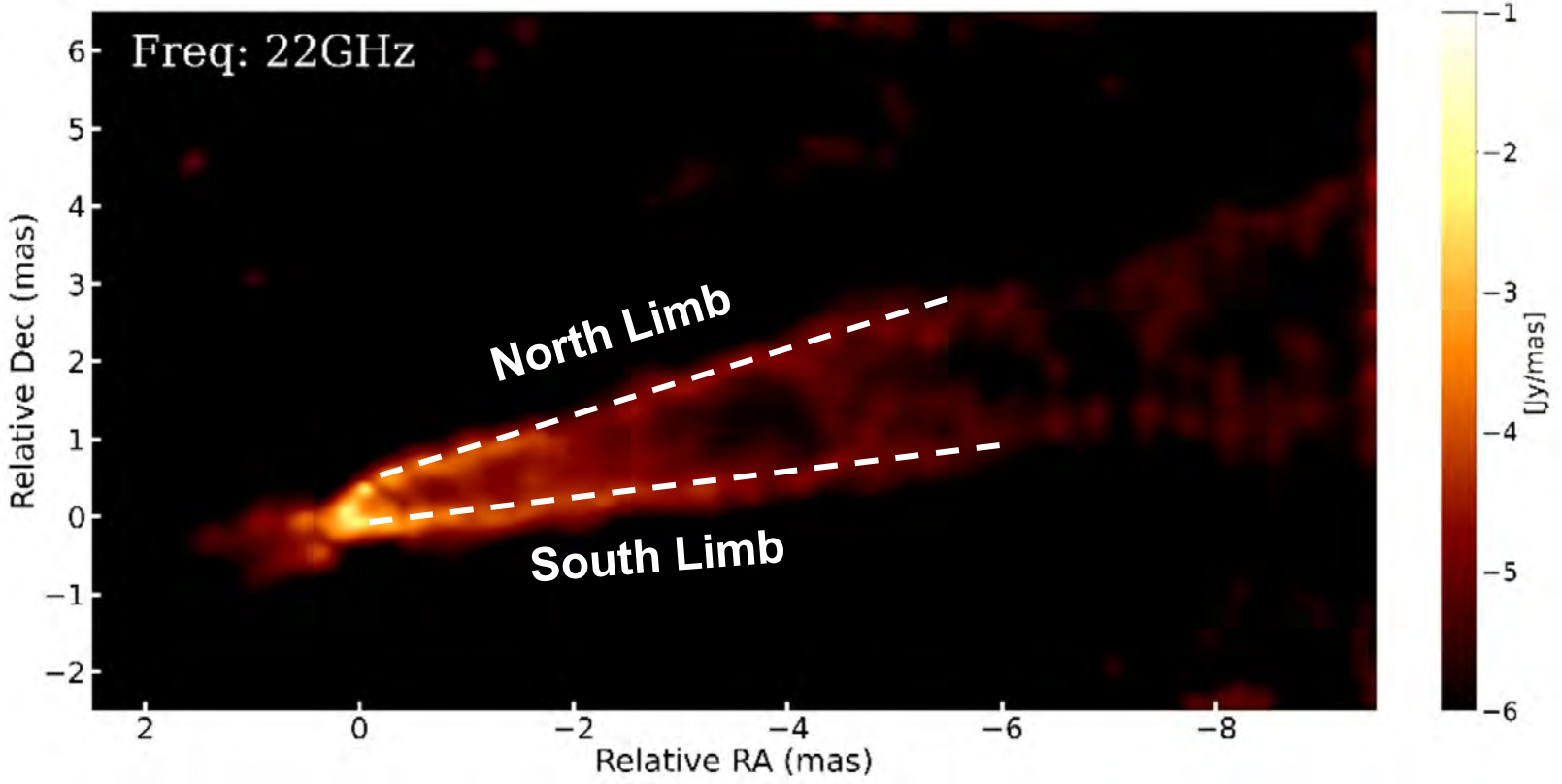


# Edge-Brightened Jet in M87

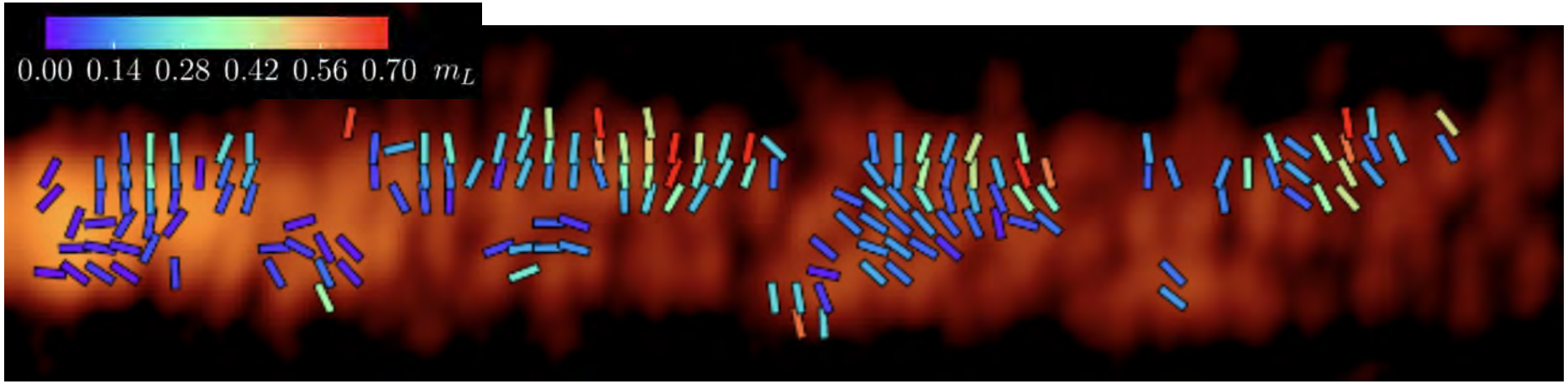
Poster



Imkwang Kang



# Results

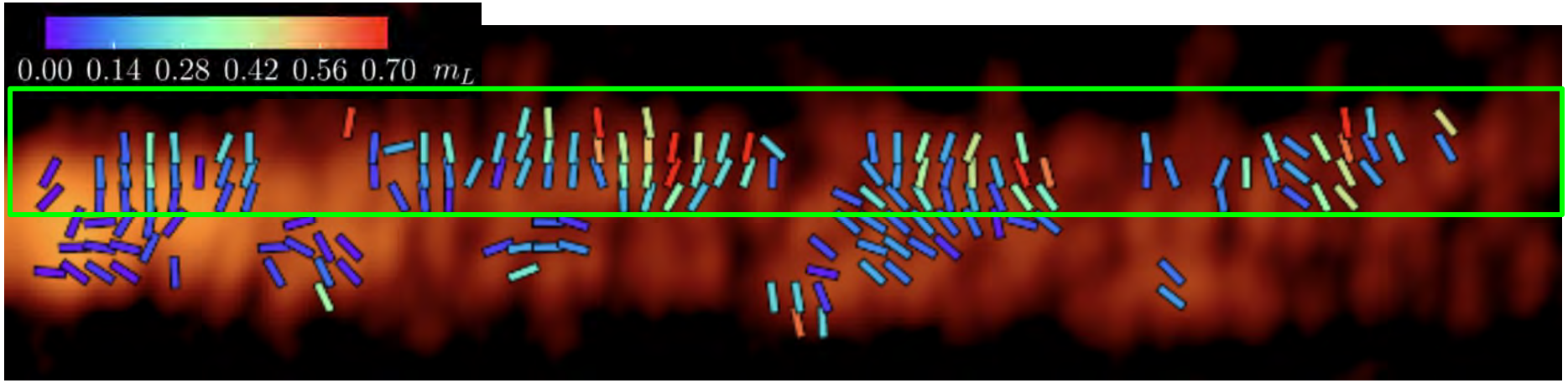



-20 mas -100 mas

In the Far Zone (between ≈ 2e4 and ≈ 2e5 Rg)

- North : EVPAs Perpendicular to the Jet Axis.
- South : EVPAs Either Parallel or Perpendicular to the Jet Axis.
- Higher Fractional Linear Polarization in the North Limb than the South Limb.

# Results

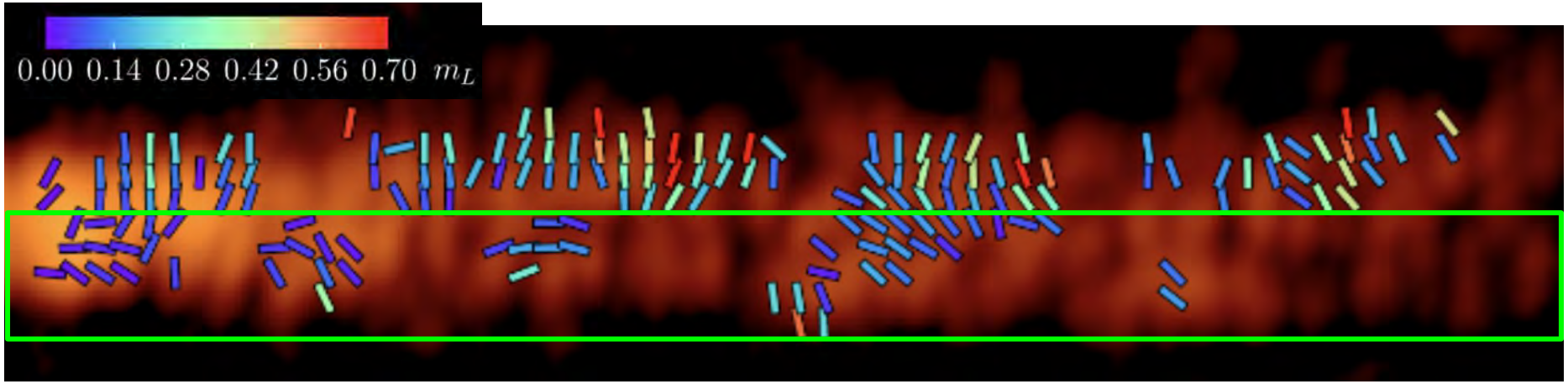



-20 mas -100 mas

In the Far Zone (between ≈ 2e4 and ≈ 2e5 Rg)

- North : EVPAs Perpendicular to the Jet Axis.
- South : EVPAs Either Parallel or Perpendicular to the Jet Axis.
- Higher Fractional Linear Polarization in the North Limb than the South Limb.

# Results

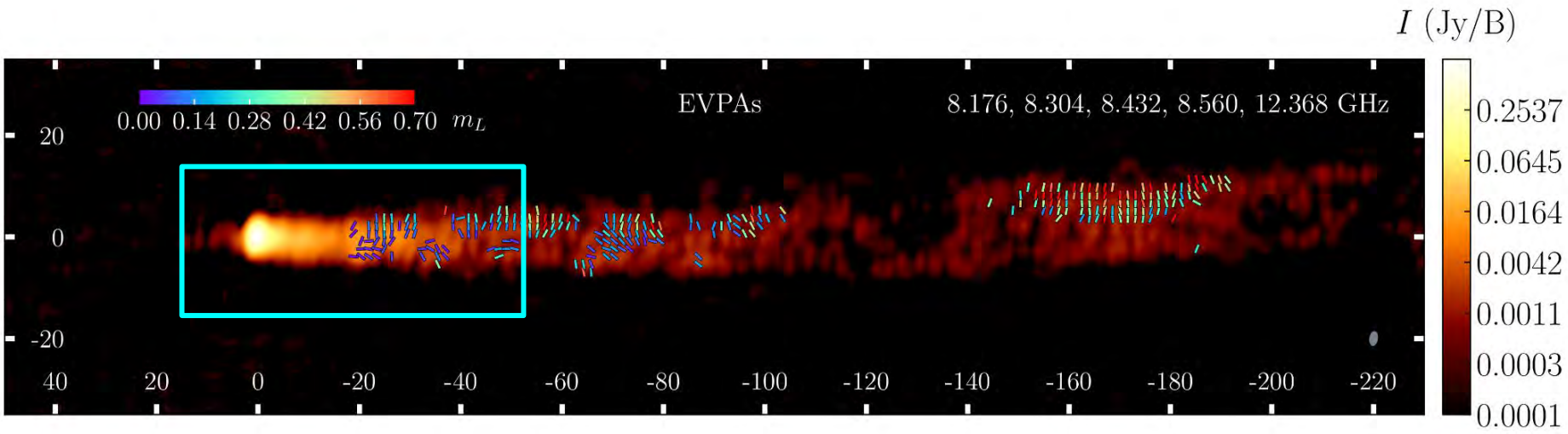



-20 mas -100 mas

In the Far Zone (between ≈ 2e4 and ≈ 2e5 Rg)

- North : EVPAs Perpendicular to the Jet Axis.
- South : EVPAs Either Parallel or Perpendicular to the Jet Axis.
- Higher Fractional Linear Polarization in the North Limb than the South Limb.

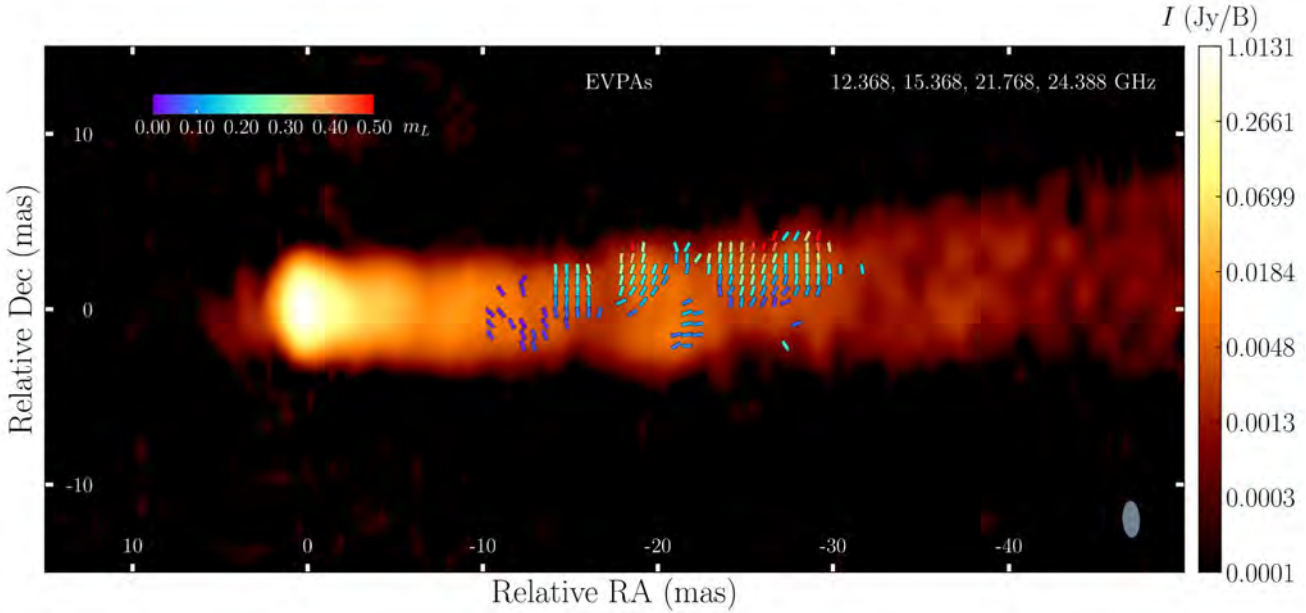
# Results




In the Far Zone (between ≈ 2e4 and ≈ 2e5 Rg)

- North : EVPAs Perpendicular to the Jet Axis.
- South : EVPAs Either Parallel or Perpendicular to the Jet Axis.
- Higher Fractional Linear Polarization in the North Limb than the South Limb.

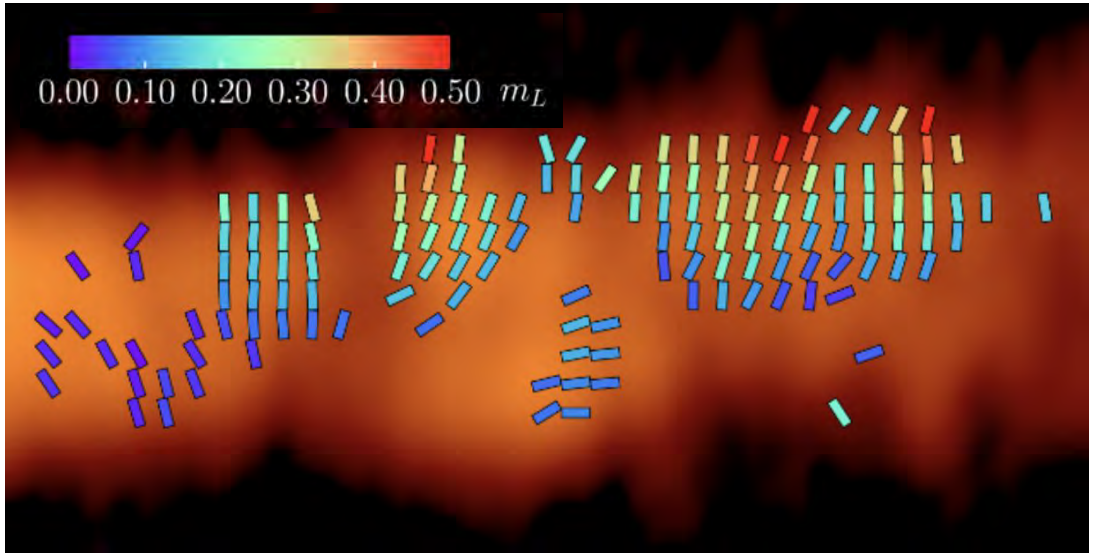
# Results




In the Near Zone (down to ≈ 3e4 Rg)

- North : EVPAs Perpendicular to the Jet Axis.
- South : EVPAs Either Parallel or Perpendicular to the Jet Axis.
- Higher Fractional Linear Polarization in the North Limb than the South Limb.

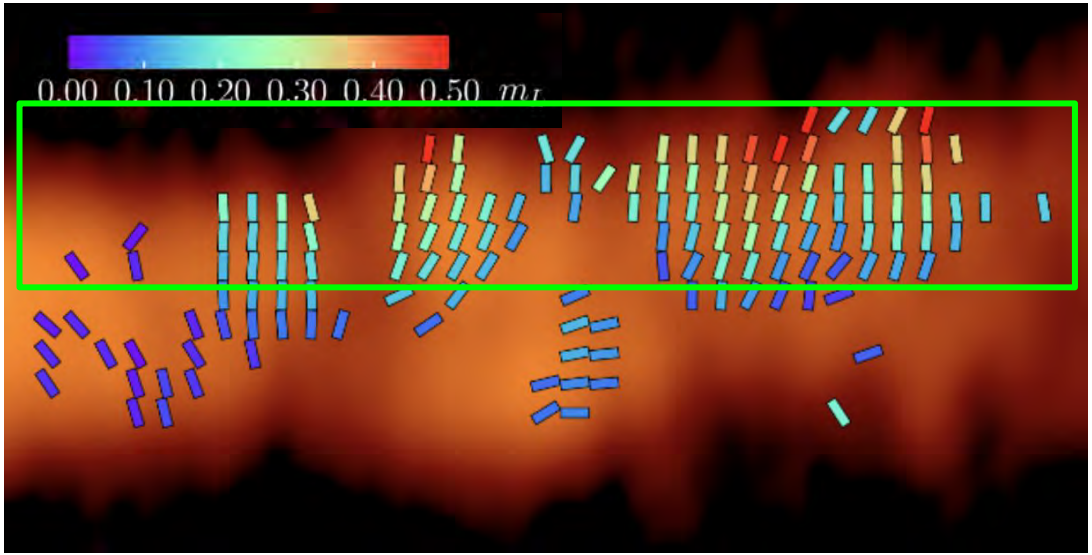
# Results




In the Near Zone (down to ≈ 3e4 Rg)

- North : EVPAs Perpendicular to the Jet Axis.
- South : EVPAs Either Parallel or Perpendicular to the Jet Axis.
- Higher Fractional Linear Polarization in the North Limb than the South Limb.

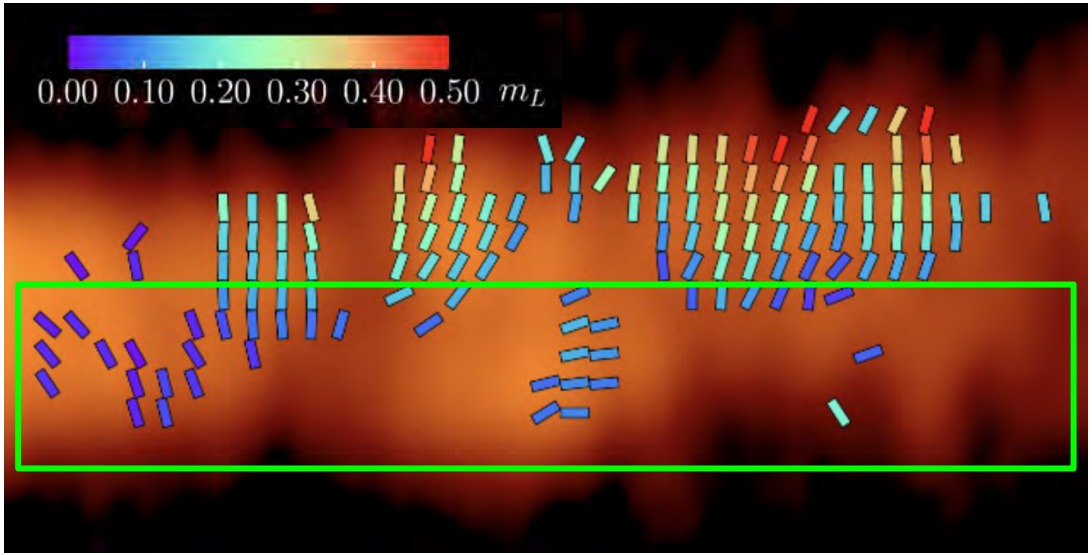
# Results




In the Near Zone (down to ≈ 3e4 Rg)

- North : EVPAs Perpendicular to the Jet Axis.
- South : EVPAs Either Parallel or Perpendicular to the Jet Axis.
- Higher Fractional Linear Polarization in the North Limb than the South Limb.

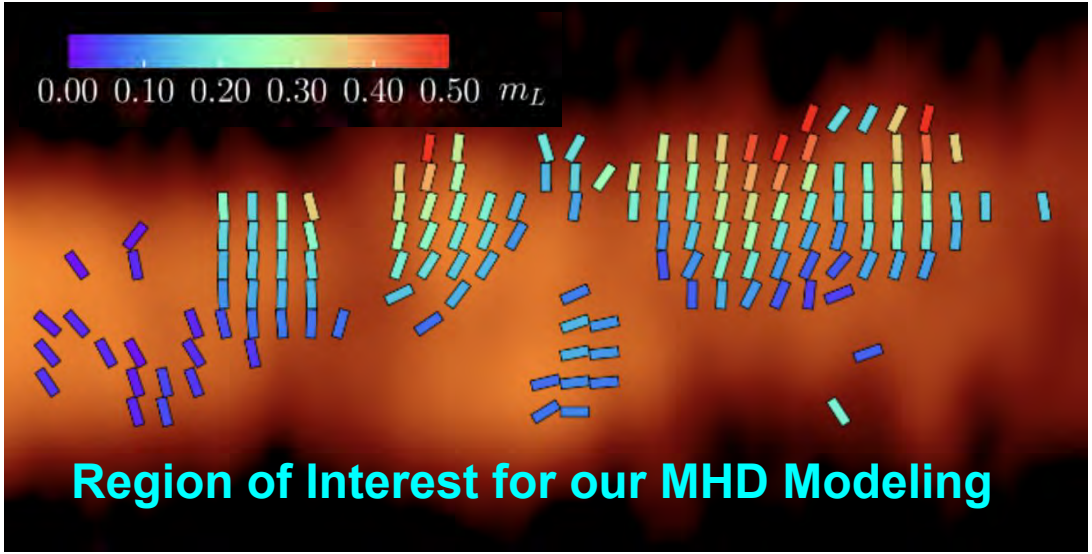
# Results




In the Near Zone (down to ≈ 3e4 Rg)

- North : EVPAs Perpendicular to the Jet Axis.
- South : EVPAs Either Parallel or Perpendicular to the Jet Axis.
- Higher Fractional Linear Polarization in the North Limb than the South Limb.

# Results




In the Near Zone (down to ≈ 3e4 Rg)

- North : EVPAs Perpendicular to the Jet Axis.
- South : EVPAs Either Parallel or Perpendicular to the Jet Axis.
- Higher Fractional Linear Polarization in the North Limb than the South Limb.

# Modeling

We would like to reproduce the three key observed features:

1. Symmetric total-intensity (Stokes I) emission.
2. Higher fractional polarization in the north limb than in the south limb.
3. EVPAs perpendicular to the jet axis in the north limb, and a mixture of parallel and perpendicular EVPAs in the south limb.

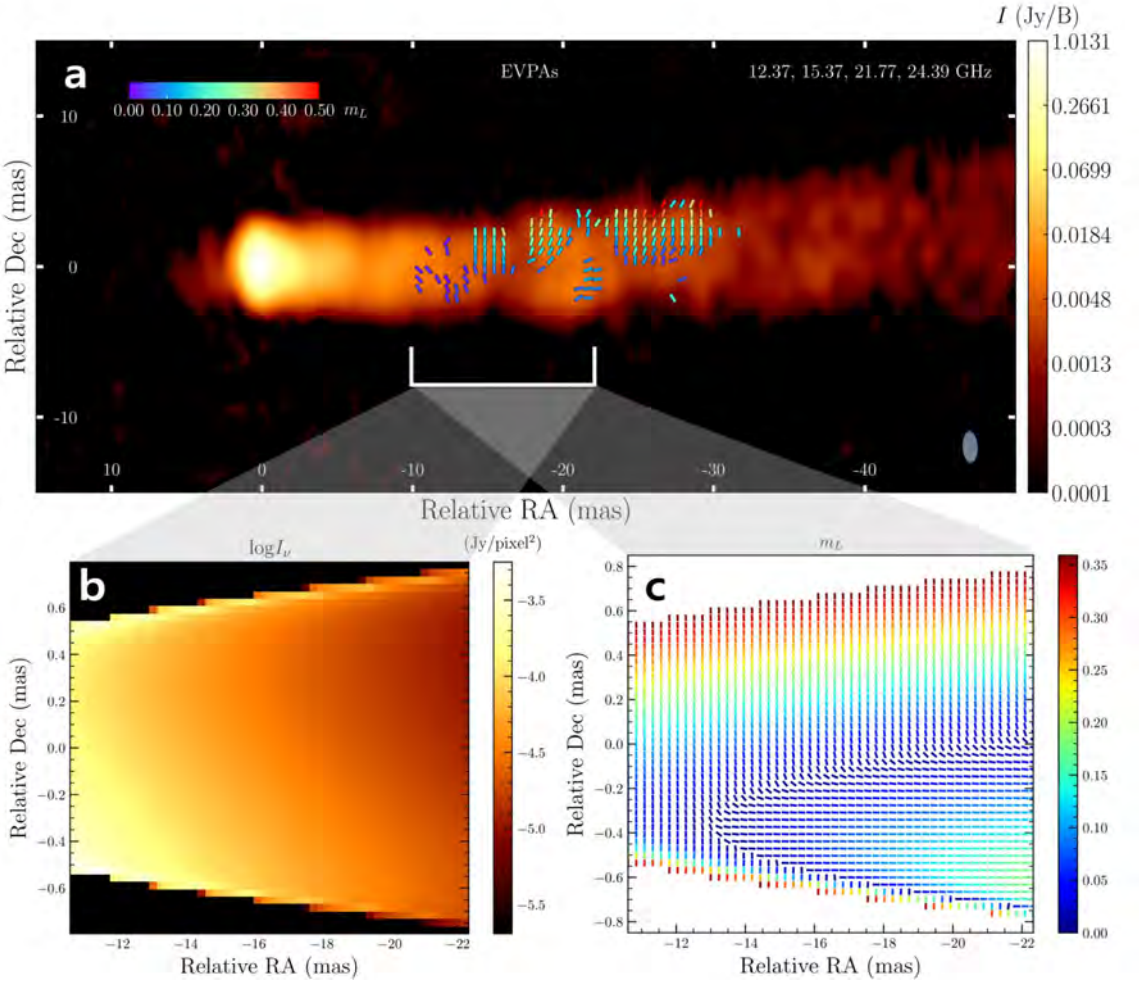
# Modeling

## Description of the model

- Evolution of the flow and magnetic field following MHD from the vicinity of the black hole to the extended jet region.
- Assume an optically thin, synchrotron-emitting jet.
- Emitting region concentrated near the jet boundary (limb brightening).
- Jet viewed at 17 degrees to the axis.
- Compute Stokes I,Q,U via polarized radiative transfer.
- Ignore Faraday rotation (images are RM-corrected).
- Include a **“dissipation layer”** upstream of the region of interest.

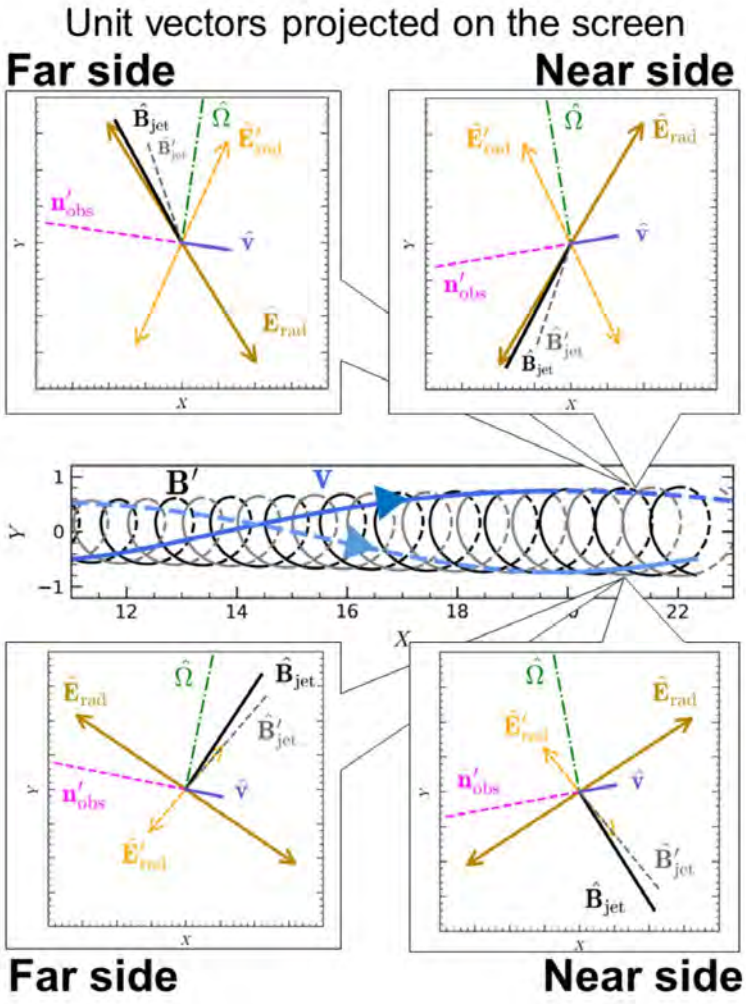
Observation

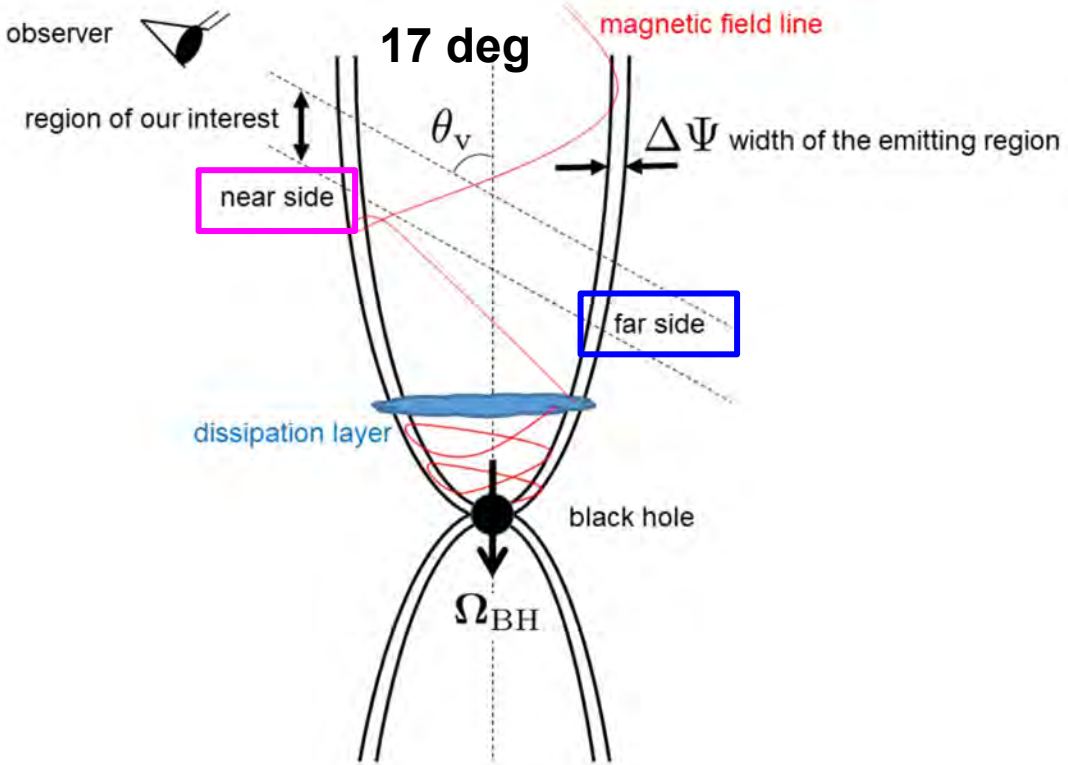
Model



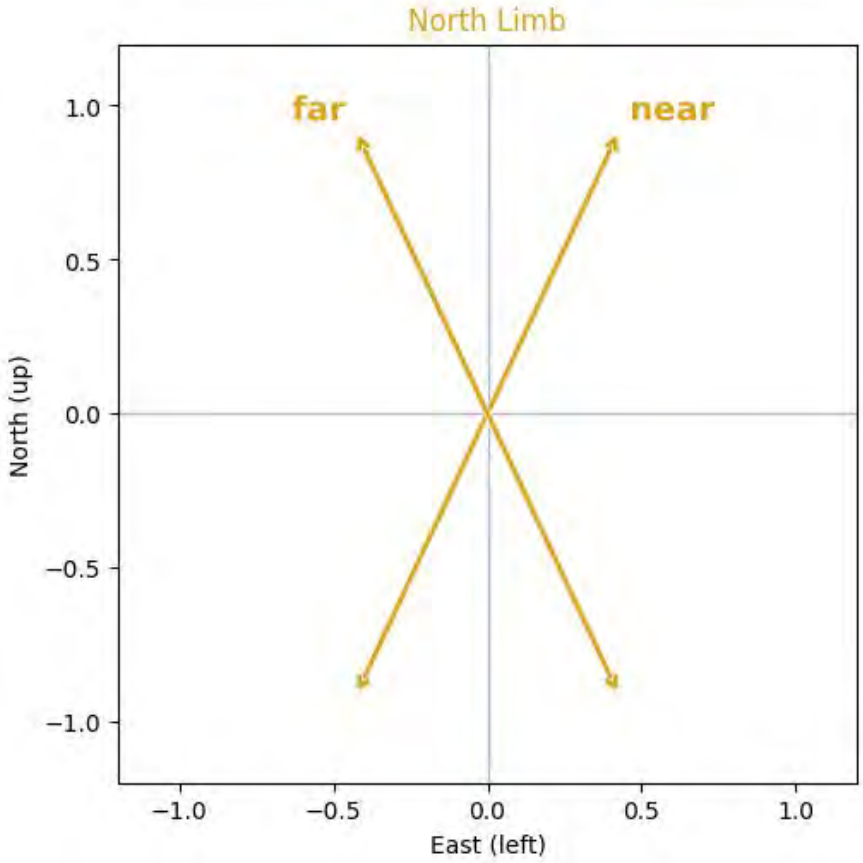

We conducted a Parameter Survey and found that a model with a comoving frame **helical-field pitch angle of 45 degrees** reproduces the three observed features.

1. Symmetric Stokes I.
2. Higher Fractional Pol. in the North Limb.
3. Perpendicular EVPAs in the North Limb and Parallel/Perpendicular EVPAs in the South Limb.

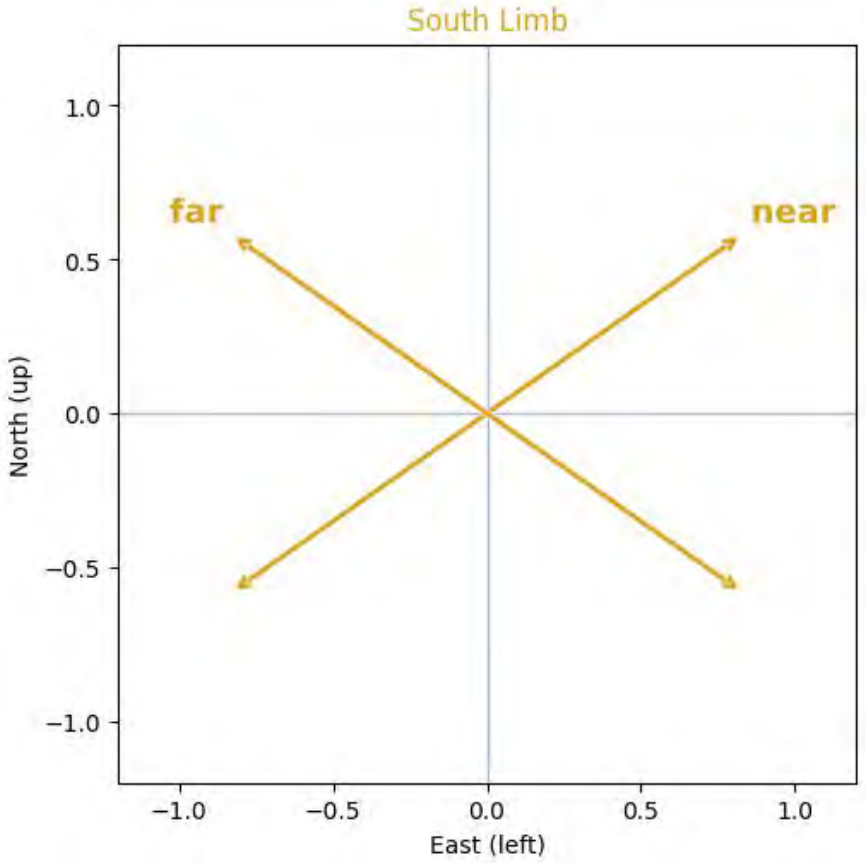

Unit vectors projected on the screen
Far side
Near side
Far side
Near side


observer
17 deg
magnetic field line
region of our interest
$\theta_v$
$\Delta\Psi$ width of the emitting region
near side
far side
dissipation layer
black hole
$\Omega_{BH}$

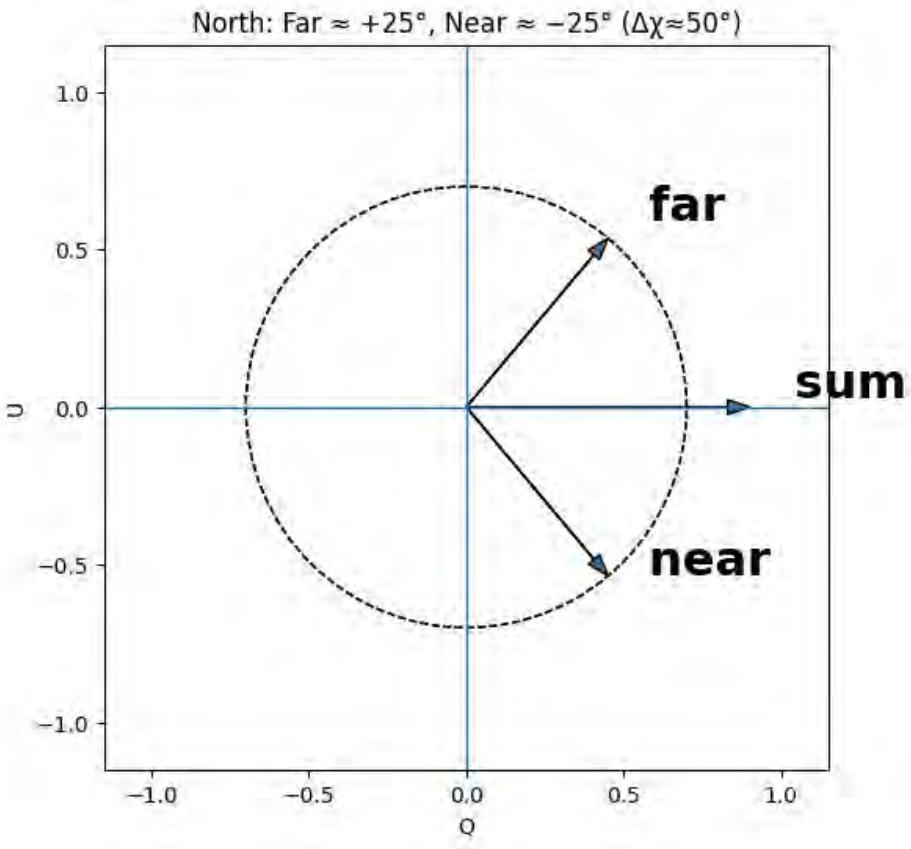
## North Limb



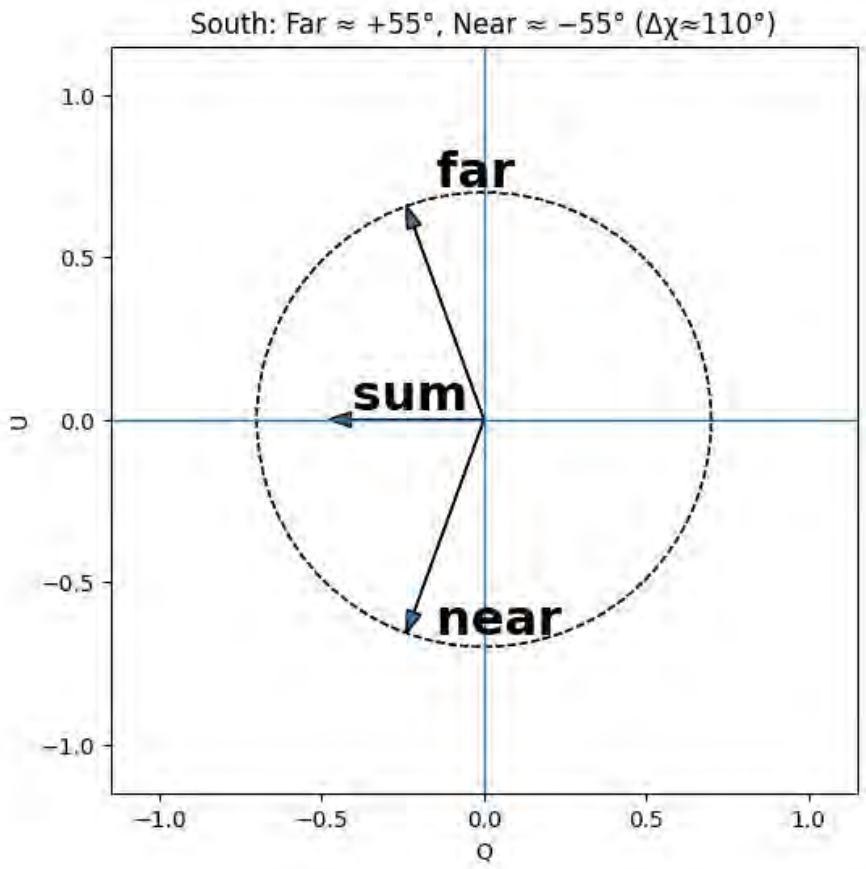

## South Limb

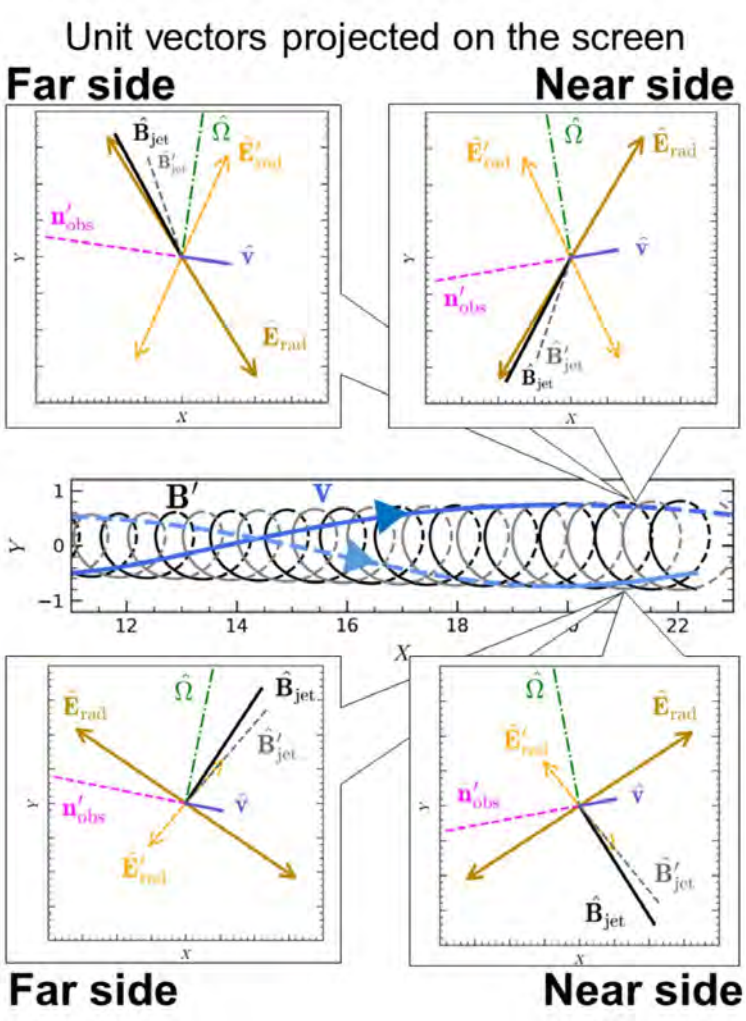


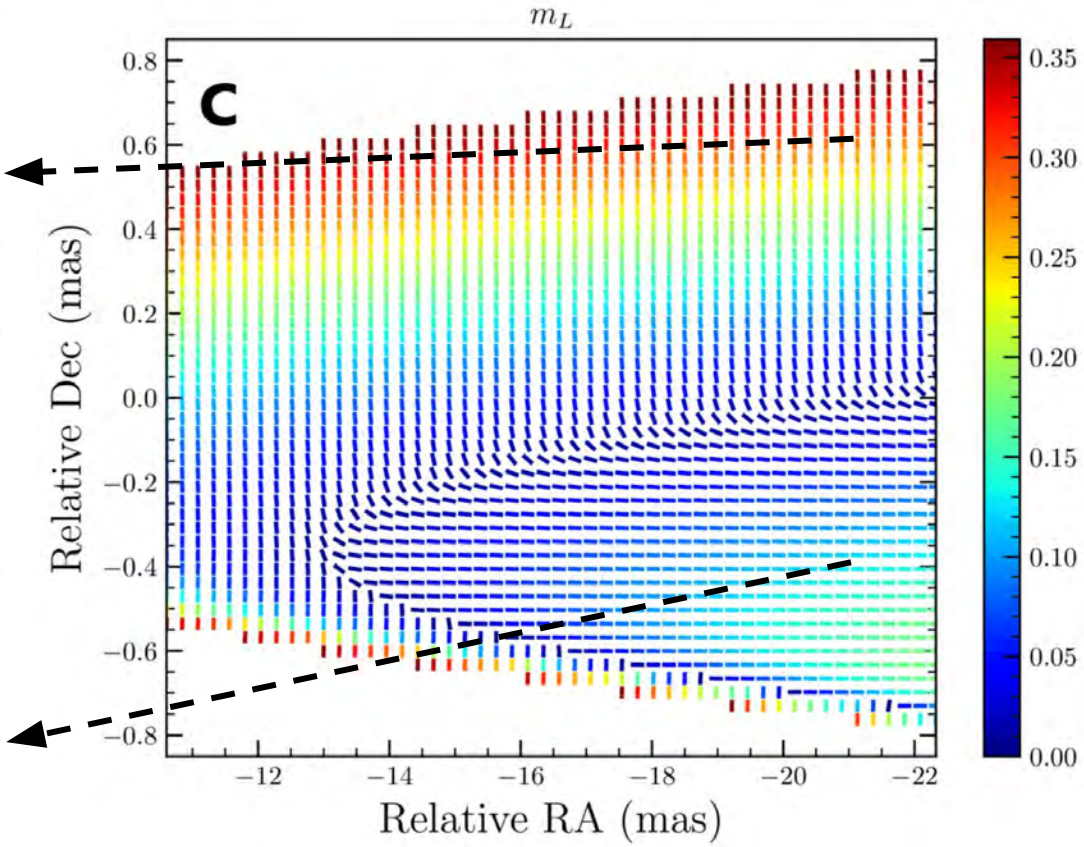
## North Limb

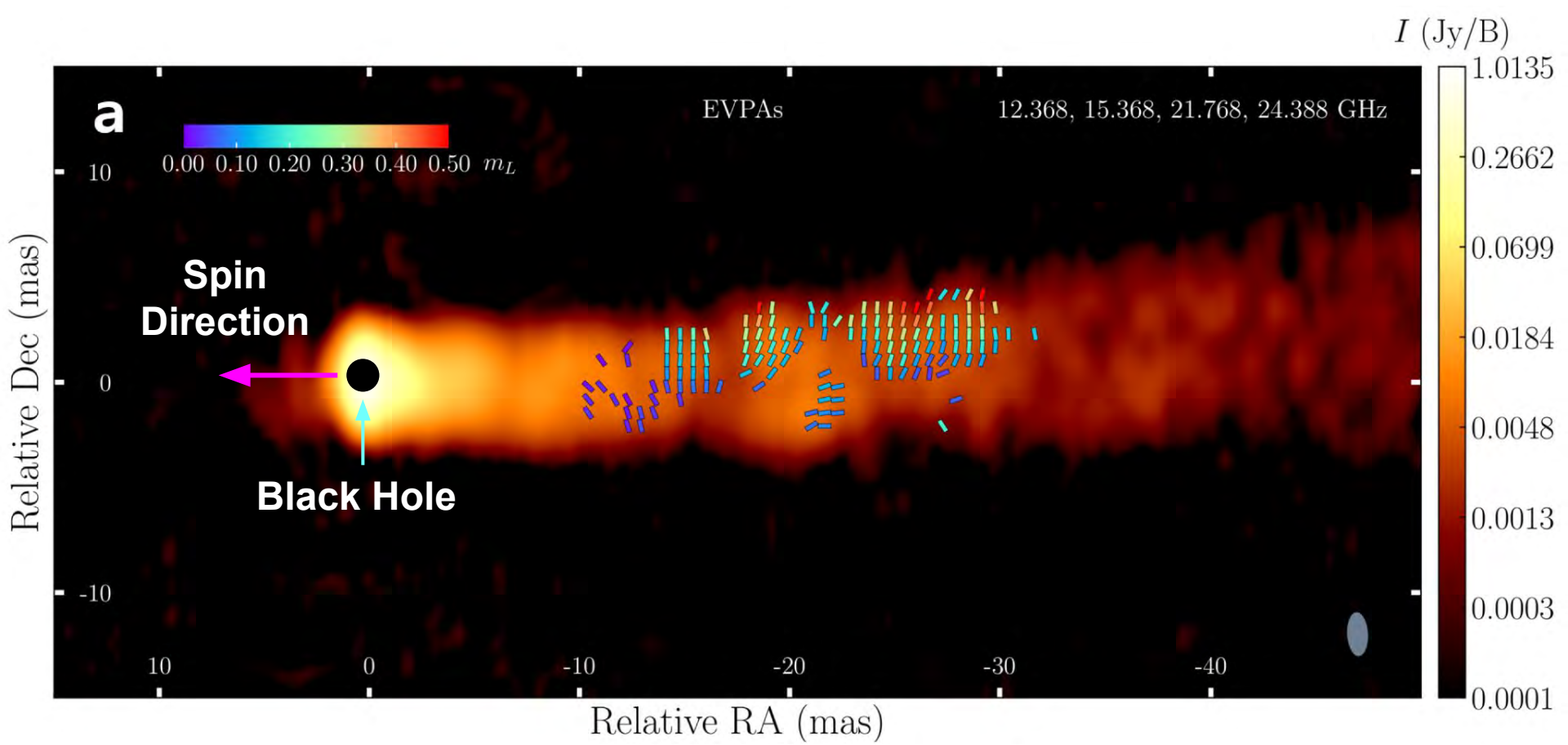



## South Limb

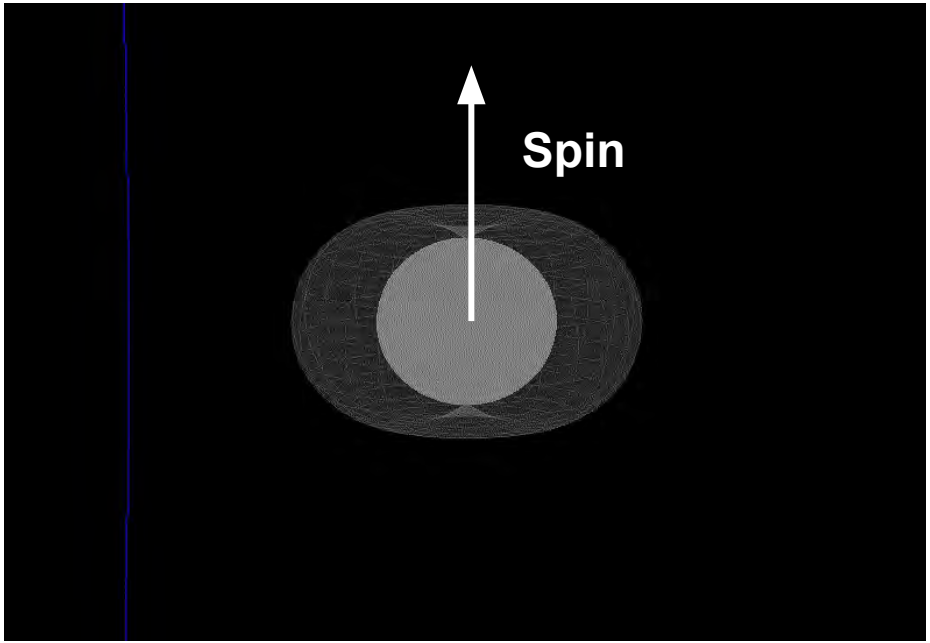


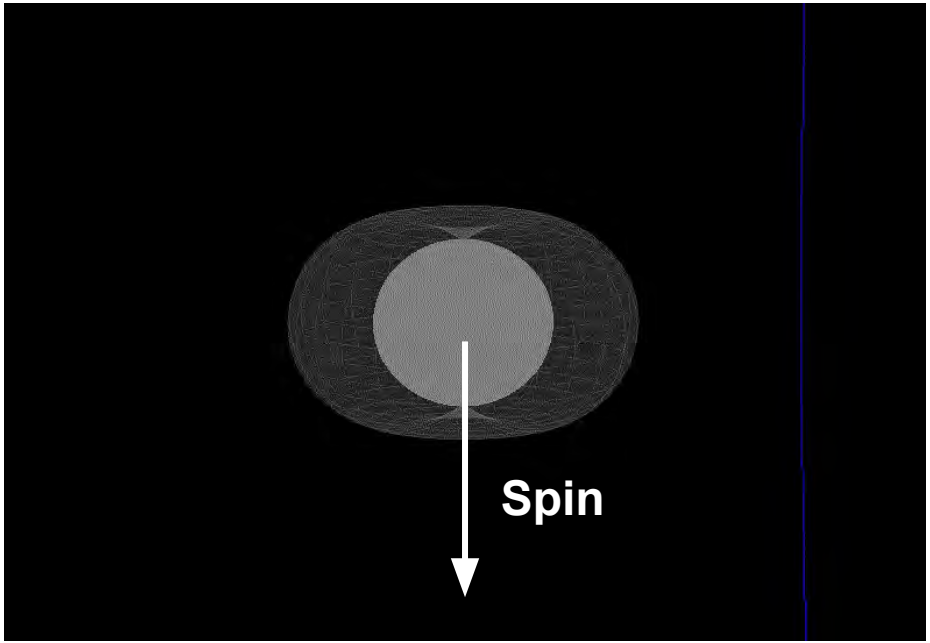

Unit vectors projected on the screen
Far side
Near side
B′
V
Far side
Near side


$m_L$
C
Relative Dec (mas)
Relative RA (mas)
0.8
0.6
0.4
0.2
0.0
−0.2
−0.4
−0.6
−0.8
−12
−14
−16
−18
−20
−22
0.35
0.30
0.25
0.20
0.15
0.10
0.05
0.00

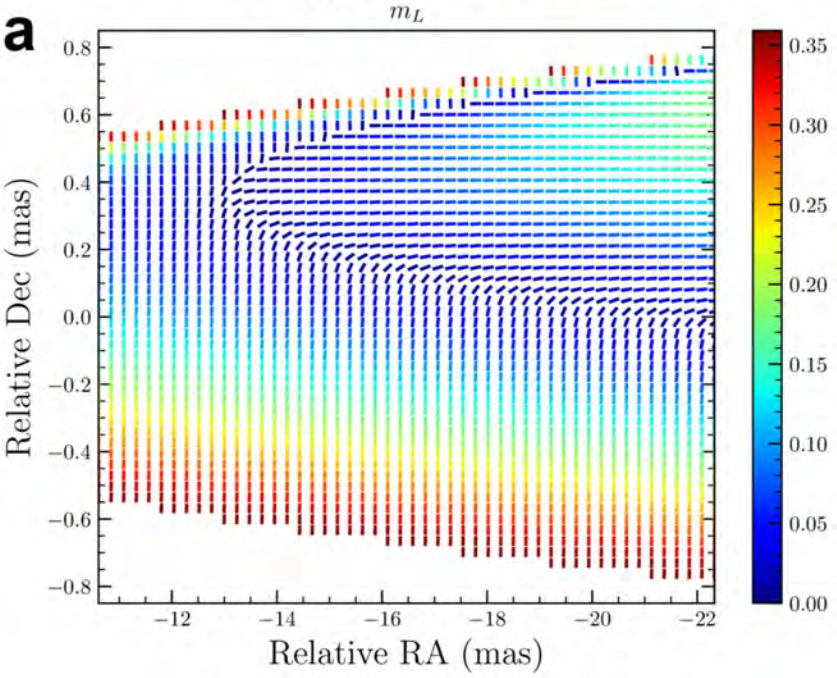

a
EVPAs
12.368, 15.368, 21.768, 24.388 GHz
0.00 0.10 0.20 0.30 0.40 0.50 $m_L$
Spin Direction
Black Hole
Relative Dec (mas)
Relative RA (mas)
10
0
-10
-20
-30
-40
$I$ (Jy/B)
1.0135
0.2662
0.0699
0.0184
0.0048
0.0013
0.0003
0.0001

Semenov (2004)

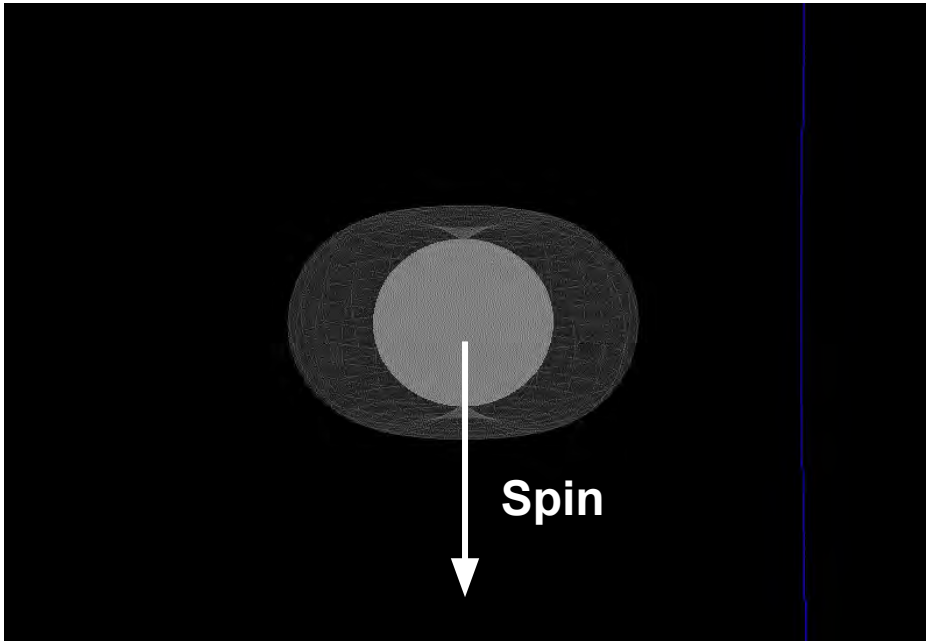


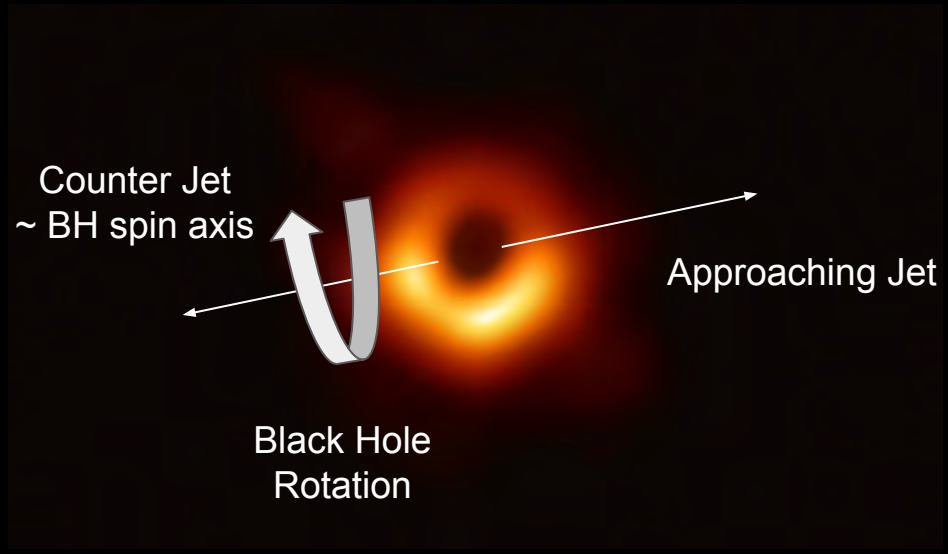
# Flipped BH spin

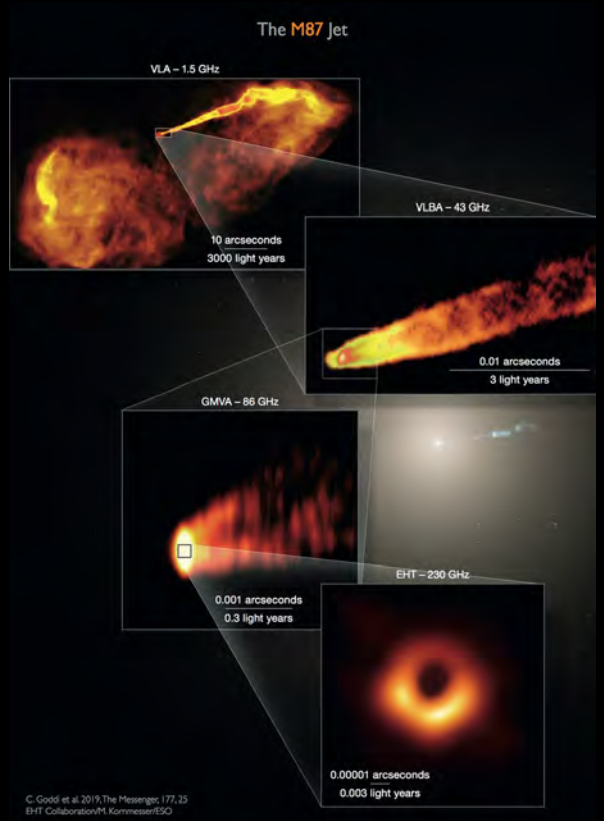



Semenov (2004)



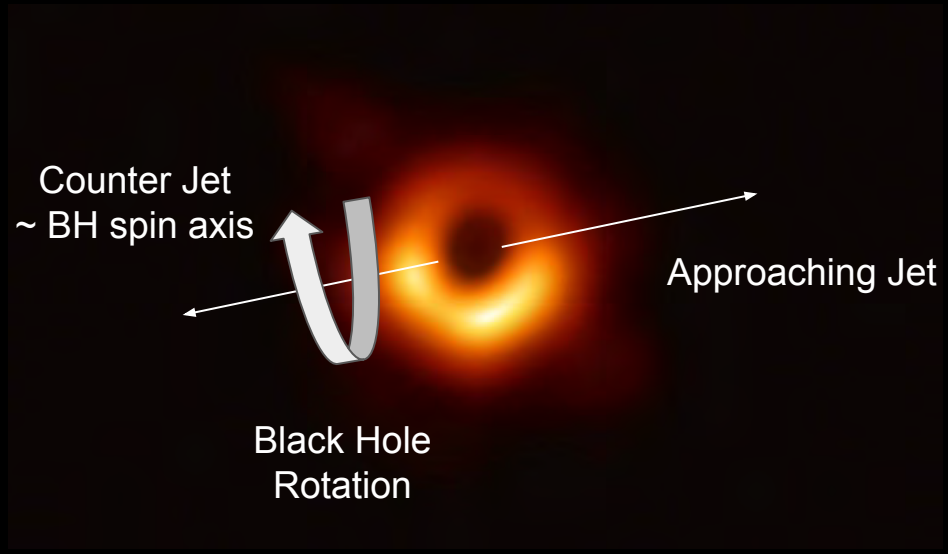
# Doppler Boosting and Brightness Asymmetry

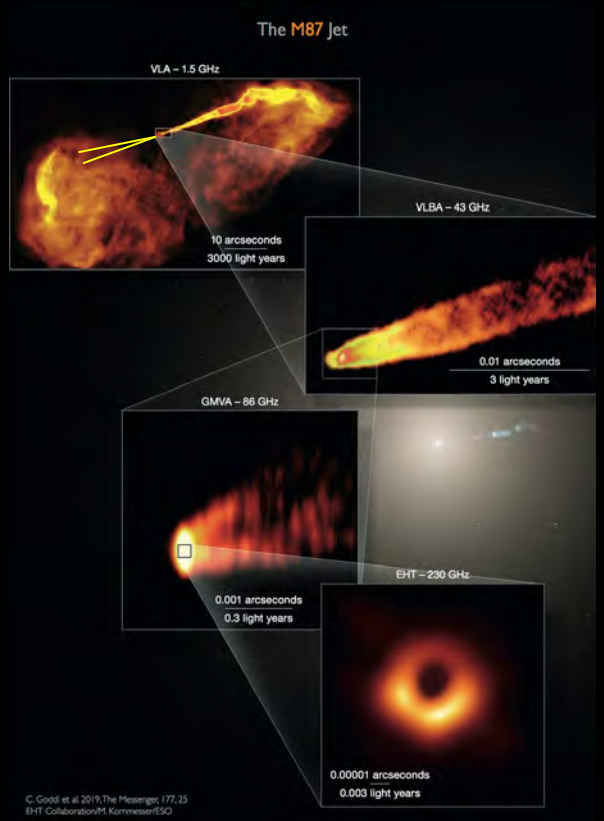



The frame-dragging and Doppler boosting effects.

# Doppler Boosting and Brightness Asymmetry

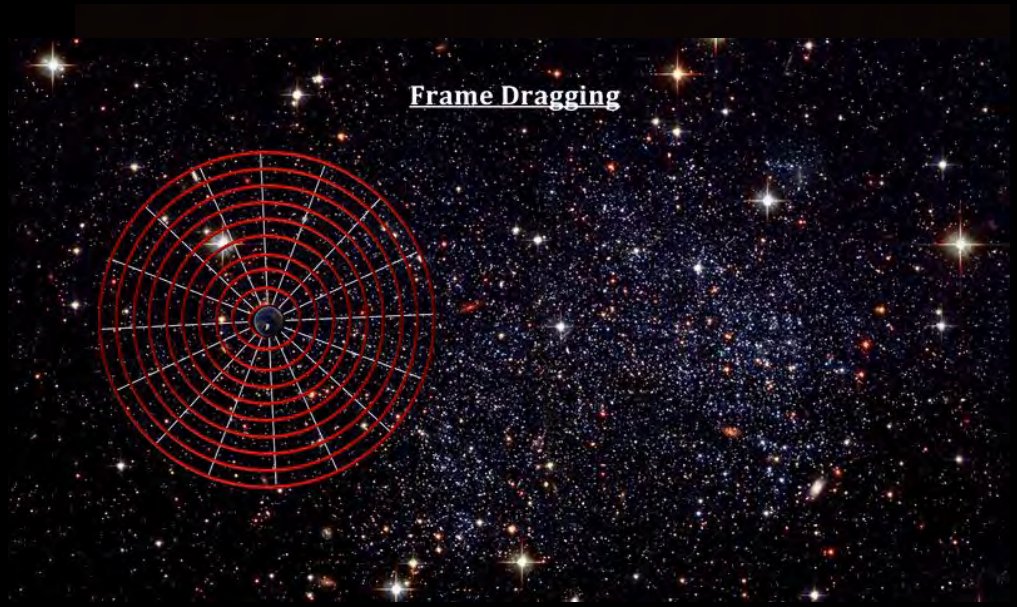


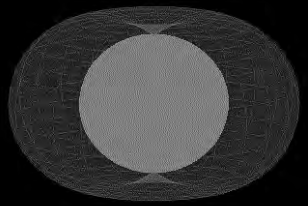




The frame-dragging and Doppler boosting effects.

# Doppler Boosting and Brightness Asymmetry

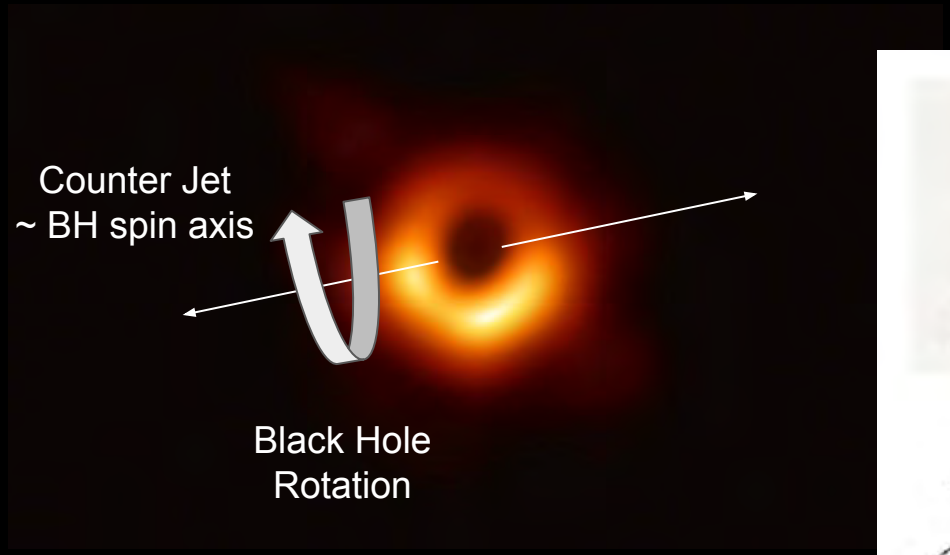
Semenov (2004)



The frame-dragging and Doppler boosting effects.

# Doppler Boosting and Brightness Asymmetry



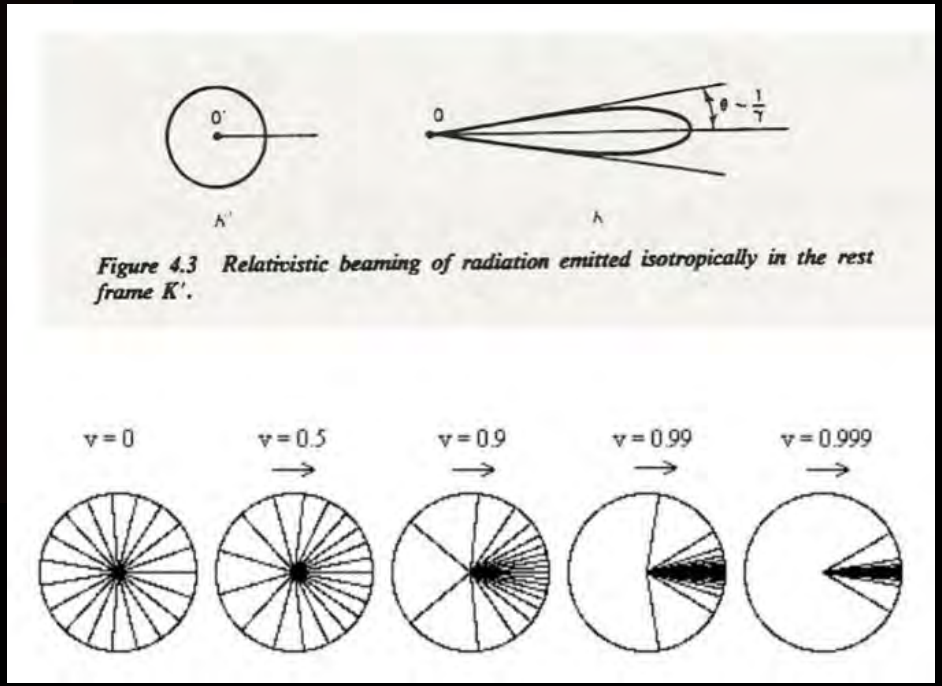
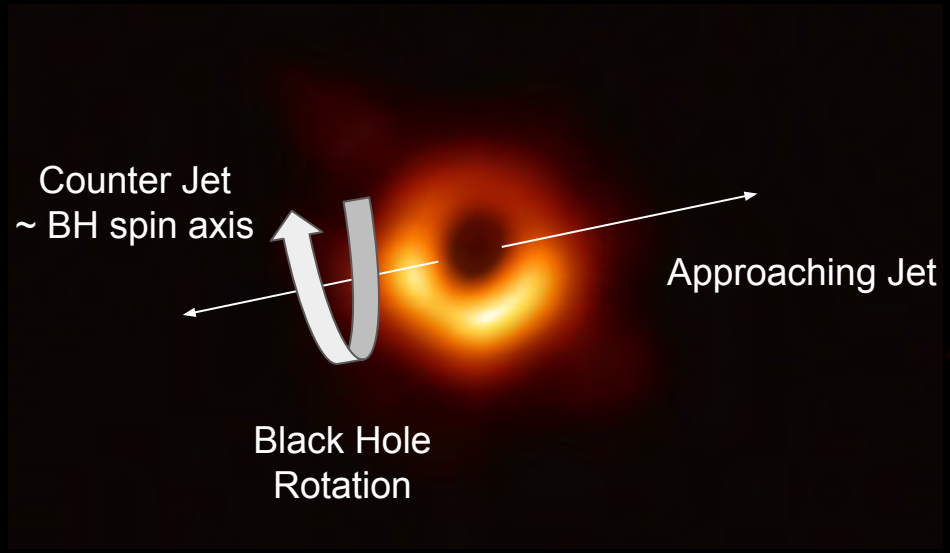




*Figure 4.3 Relativistic beaming of radiation emitted isotropically in the rest frame K'.*

The frame-dragging and Doppler boosting effects.

# Doppler Boosting and Brightness Asymmetry

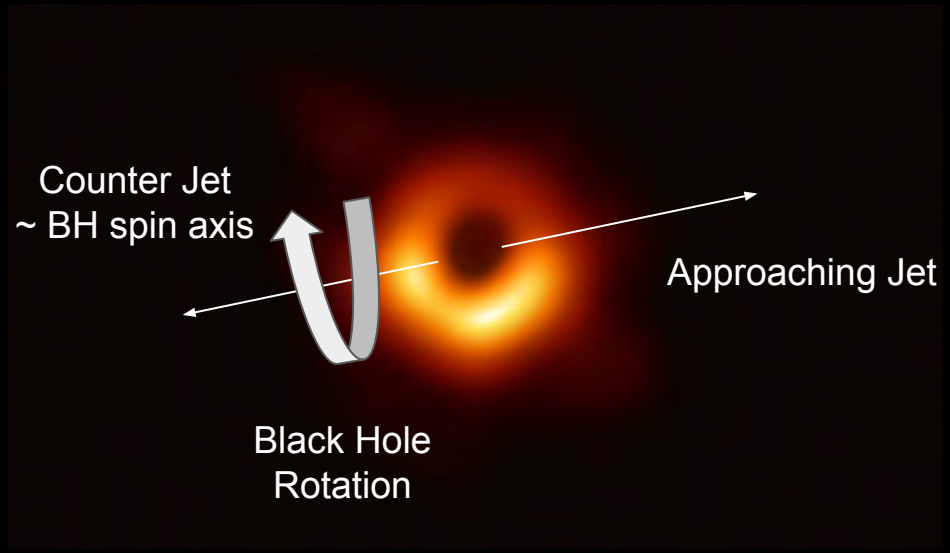



Interstellar (2014)



The frame-dragging and Doppler boosting effects.

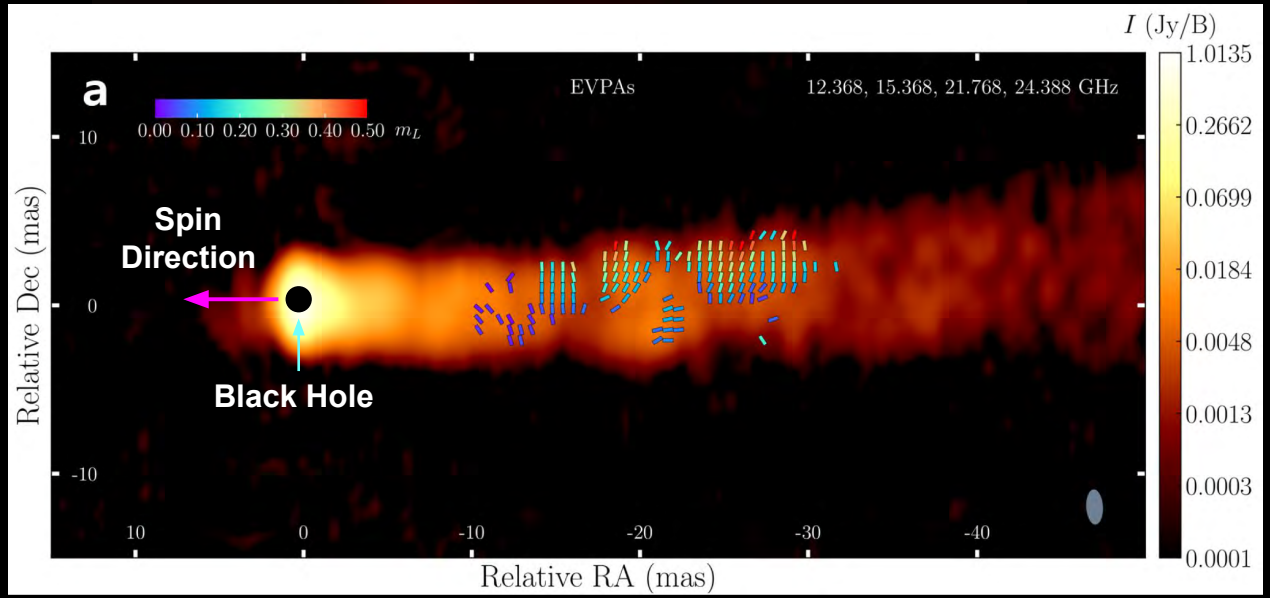
# Doppler Boosting and Brightness Asymmetry

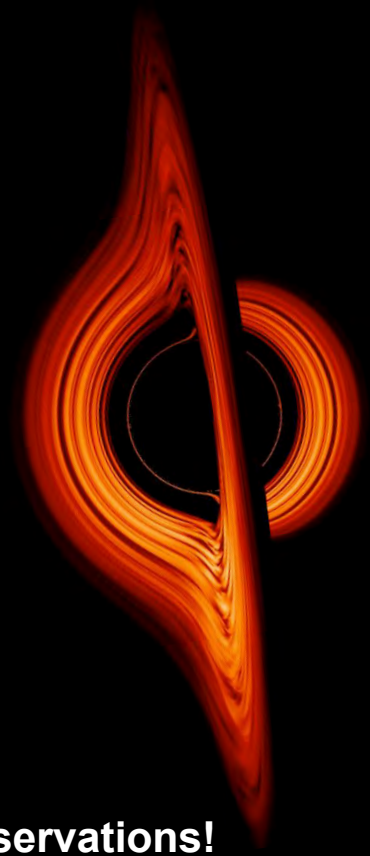





The frame-dragging and Doppler boosting effects.

# Doppler Boosting and Brightness Asymmetry



**Consistent with the BH spin direction inferred from the EHT observations!**

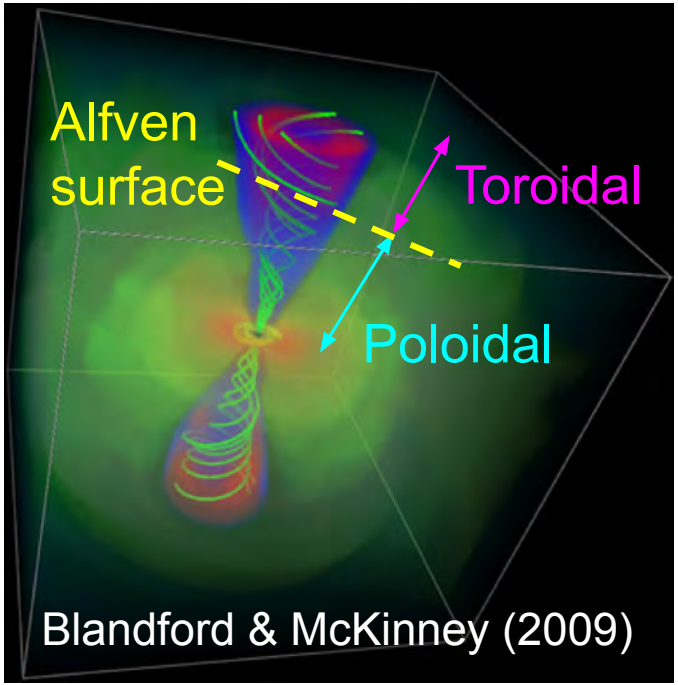
# Discussion

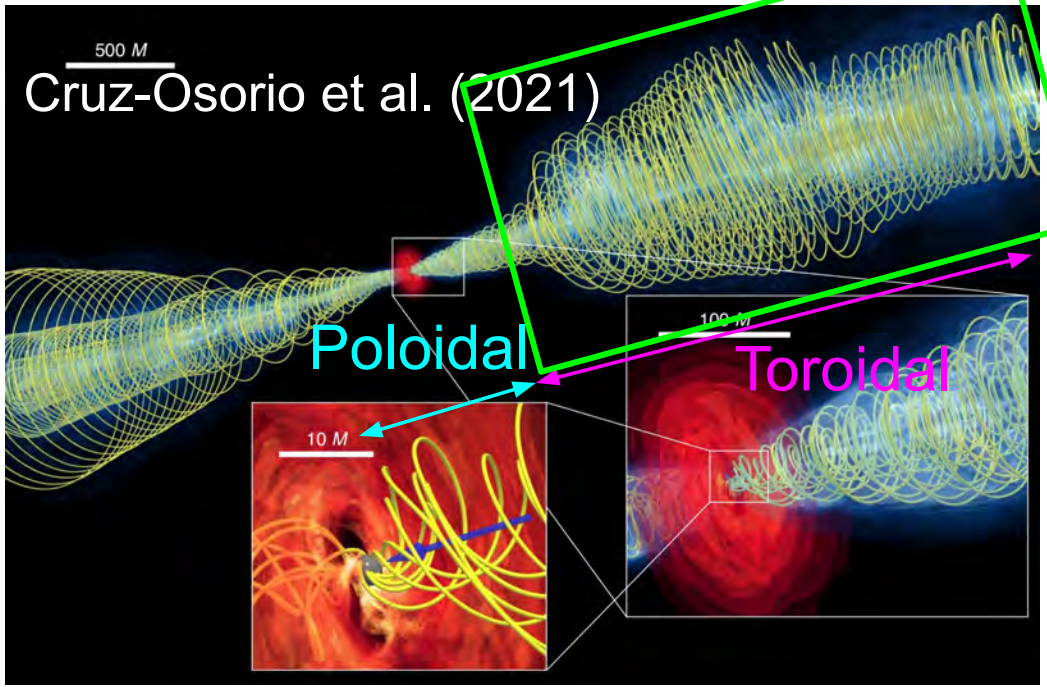
Our model suggests the presence of a helical magnetic field with a rest-frame pitch angle of 45 degrees.

$$|B_\phi / B_p| \approx R/R_L > 37$$ : according to the MHD model without dissipation

$$|B_\phi / B_p| \approx |B'_\phi / B'_p| \times \Gamma \sim 5.6$$ : constrained by our data

# Theory Prediction: Poloidal to Toroidal B-Field Transition




Current MHD theory predicts a **toroidal-dominated B-field** structure in most of the ACZ regions of AGNs.

# Discussion

Our model suggests the presence of a helical magnetic field with a rest-frame pitch angle of 45 degrees.

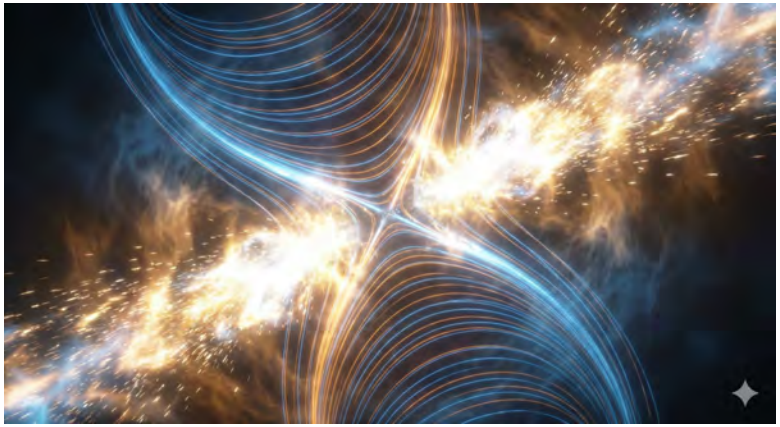
$$|B_\phi/B_p| \approx R/R_L > 37$$ : according to the MHD model without dissipation

$$|B_\phi/B_p| \approx |B'_\phi/B'_p| \times \Gamma \sim 5.6$$ : constrained by our data

→ suggest significant dissipation of the toroidal magnetic field is required.
Potential Mechanisms: current-driven kink instability, magnetic reconnection, shear acceleration, and mass loading onto the jets from the surrounding medium.



Current-Driven Kink Instability



Magnetic Reconnection



Velocity Shear



Mass-Loading from the Ambient

# Discussion

Our model suggests the presence of a helical magnetic field with a rest-frame pitch angle of 45 degrees.

$$|B_\phi/B_p| \approx R/R_L > 37$$ : according to the MHD model without dissipation

$$|B_\phi/B_p| \approx |B'_\phi/B'_p| \times \Gamma \sim 5.6$$ : constrained by our data

→ suggest significant dissipation of the toroidal magnetic field is required.
Potential Mechanisms: current-driven kink instability, magnetic reconnection, shear acceleration, and mass loading onto the jets from the surrounding medium.

→ $B_p \propto R^{-2},\ B_\phi \propto R^{-1}$ do not hold for the jet ACZ.

# Summary

Paper Accepted in ApJL, arXiv: 2511.13008

